

OPTIMAL REGULARIZATION FOR PERFORMATIVE LEARNING

Edwige Cyffers

Institute of Science and Technology Austria
Klosterneuburg, Austria
edwige.cyffers@ist.ac.at

Alireza Mirrokni

Sharif University of Technology
Tehran, Iran
alirezamirrokni28@gmail.com

Marco Mondelli

Institute of Science and Technology Austria
Klosterneuburg, Austria
marco.mondelli@ist.ac.at

ABSTRACT

In performative learning, the data distribution reacts to the deployed model—for example, because strategic users adapt their features to game it—which creates a more complex dynamic than in classical supervised learning. One should thus not only optimize the model for the current data but also take into account that the model might steer the distribution in a new direction, without knowing the exact nature of the potential shift. We explore how regularization can help cope with performative effects by studying its impact in high-dimensional ridge regression. We show that, while performative effects worsen the test risk in the population setting, they can be beneficial in the over-parameterized regime where the number of features exceeds the number of samples. We show that the optimal regularization scales with the overall strength of the performative effect, making it possible to set the regularization in anticipation of this effect. We illustrate this finding through empirical evaluations of the optimal regularization parameter on both synthetic and real-world datasets.

1 INTRODUCTION

When machine learning predictions affect user outcomes, deployed models can induce shifts in the data distribution. These shifts may result from strategic user behavior—where individuals try to secure favorable outcomes such as loan approval or college admission (Bechavod et al., 2021; Narang et al., 2023; Wang et al., 2023)—or from self-fulfilling prophecies, for example in economic forecasts, recommendation systems, or predictive policing (Morgenstern, 1928; Ensign et al., 2018; Ursu, 2015). Such distribution shifts can undermine predictive performance over time, amplifying bias and reducing model quality (Taori & Hashimoto, 2023; Pan et al., 2024). Performative learning (Perdomo et al., 2020) addresses this feedback loop by parameterizing the data distribution with the same parameter as the model. This allows optimization to account not only for the training loss but also for the steering of the data distribution.

Unfortunately, while optimizing model parameters is a classical problem in machine learning, estimating the performative effect on the distribution is generally infeasible, as the distribution is unknown to the learner. Several algorithms have been proposed to approximate this effect (Miller et al., 2021; Izzo et al., 2022; Cyffers et al., 2024), typically by assuming that it depends on a small number of parameters in a sufficiently simple way that can be learned across the first few deployments. However, these methods are limited to relatively toy examples in small dimensions and may be impractical in real-world settings. In particular, many approaches require numerous repeated deployments, alternating between loss minimization and distribution steering. Yet in practice, deployment often happens only once after full training. This makes repeated risk minimization (RRM) (Perdomo et al., 2020)—where one trains until convergence before deployment, and the number of deployments is small—the default in many applications, even though it remains largely unaddressed

by existing mitigation methods. This motivates a shift away from exact estimation of performative effects toward the study of principled choices of loss functions and models, and in particular regularization is a natural and tractable candidate.

In this work, we study how regularization mitigates performative effects in repeated retraining. Unlike estimation-based methods, regularization does not depend on a precise characterization of the distribution shift, avoids their limitations, and introduces little computational overhead. Prior work suggests its potential benefits: Perdomo et al. (2020) proved that retraining converges to an optimal solution under assumptions tied to the strong convexity of the loss, which ridge regularization can enforce; more recently, Cyffers et al. (2024) showed that, in classification, the performative optimum can be interpreted as a regularized version of the non-performative problem, with numerical evidence that ridge penalties perform well in small-dimensional classification tasks. A natural limitation, however, is that regularization may encourage reliance on spurious features (Bombari & Mondelli, 2025), especially when such features are reinforced by performativity.

To better understand these tradeoffs, we study the role of ridge regularization in linear regression in the presence of performativity and spurious features. We consider both *(i)* the population regime, with enough data to recover exactly the unknown vector of regression coefficients at each deployment, and *(ii)* the over-parameterized regime, where the number of data samples is a fixed fraction of the number of parameters. This last setting, though simple, captures behaviors relevant to deep learning, such as double descent (Belkin et al., 2019; Hastie et al., 2022), benign overfitting (Bartlett et al., 2020) and adversarial robustness (Fawzi et al., 2018; Ribeiro et al., 2023). In performative learning, it also brings the additional advantage that parameters and data live in the same space, simplifying the encoding of performative effects. The theoretical framework we develop enables us to provide strong evidence for the effectiveness of regularization under performativity, and to show how regularization should be scaled. More precisely, our contributions are summarized below.

1. In the population regime, we characterize how the risk depends on magnitude and direction of the performative effect, as well as on spurious features (Theorem 1). We find that the optimal regularization is proportional to the strength of the performative effect and it mitigates the performance loss due to performativity: zero excess risk can be achieved with identity covariance and constant entries of the performative vector, while the risk remains significant in the presence of a complex covariance structure and highly variable entries of the performative vector (Corollary 2).
2. In the proportional regime with random data, we establish a deterministic equivalent of the performative fixed point, depending only on population covariance and regularization (Theorem 3). The analysis of this deterministic equivalent then unveils a remarkable phenomenology: for small noise variance, the optimal regularization moves in the same direction as the performative effect on the predictive features, while it moves in the opposite direction as the performative effect on the spurious features; remarkably, the optimally-regularized risk improves in the presence of a performative effect that reinforces existing trends.
3. We illustrate these behaviors both on synthetic data and real-world dataset (Housing, LSAC).

2 RELATED WORK

Performative learning. Performative learning was introduced by Perdomo et al. (2020), where retraining was also shown to converge under assumptions including strong convexity. Subsequent works demonstrate that retraining can sometimes enable adaptation over time (Li et al., 2022; Drusvyatskiy & Xiao, 2023) but also fail dramatically (Miller et al., 2021; Izzo et al., 2022; Cyffers et al., 2024). The role of model choice has not yet been studied in performative learning, although it has been examined in the related setting of collective action (Ben-Dov et al., 2024). Interestingly, Bechavod et al. (2021) observed that performativity can, in some cases, even improve performance, and our work provides further evidence supporting this claim.

High-dimensional regression and role of ridge regularization. The high-dimensional setting where the numbers of features and samples are large and scale proportionally was considered by a rich line of work: the test error of ridgeless and ridge regression is characterized in (Hastie et al., 2022; Wu & Xu, 2020; Richards et al., 2021; Tsigler & Bartlett, 2023), with Cheng & Montanari (2024) going even beyond the proportional regime; max-margin classification is studied in (Montanari et al., 2025; Deng et al., 2022), model compression in (Chang et al., 2021), distribution shift in

(Patil et al., 2024; Mallinar et al., 2024), transfer learning in (Yang et al., 2025; Song et al., 2024) and learning from surrogate data in (Ildiz et al., 2025; Kolossov et al., 2024; Jain et al., 2024). The role of ridge regularization was also investigated, with Hastie et al. (2022) optimally tuning the ridge and Richards et al. (2021) giving conditions for the optimality of ridgeless interpolation. The sign of the optimal ridge penalty was studied for the standard in-distribution regression setup (Wu & Xu, 2020; Tsigler & Bartlett, 2023), as well as out-of-distribution (Patil et al., 2024): these works give conditions under which the optimal ridge is negative, associating the phenomenon of negative optimal regularization to over-parameterization. Our paper shows that such a phenomenon occurs also in the population setting, due to performative effects. The distribution of the empirical risk minimizer was established in (Han & Xu, 2023). Leveraging this characterization, spurious correlations were studied by Bombari & Mondelli (2025) and weak-to-strong generalization by Ildiz et al. (2025). We will also build on these tools to analyze the risk of repeated risk minimization.

3 PRELIMINARIES AND PROBLEM SETUP

In this section, we introduce our performative regression setting. We consider a sequence of model deployments $(\theta_k)_k$, and let $\mathcal{D}(\theta)$ be the dataset generated in reaction to the deployment of θ . At each deployment, n new samples are collected, and the model is fully retrained. This setting, known as repeated risk minimization (RRM) (Perdomo et al., 2020), reflects real-world scenarios where deployments are costly and thus limited in number. It also aligns with the fact that convergence to the fixed point is fast and requires only a few iterations to reach equilibrium in practice. We encode the performative effect as a shift in the label, where each feature's contribution varies depending on an additional linear term in the model parameter. This is formalized below.

Assumption 1 (Regression performative model). For $\theta \in \mathbb{R}^p$, samples from $\mathcal{D}(\theta)$ are taken i.i.d. with features $x \sim \mathcal{N}(0, \Sigma)$ drawn independently of θ and with the label y given by

$$y = x^\top \theta_{\text{pop}}^* + x^\top D\theta + w, \quad w \sim \mathcal{N}(0, \sigma^2). \quad (1)$$

We assume $p = 2d$, $(\theta_{\text{pop}}^*)^\top = (a^\top, 0)$ with a having covariance I_d/d , and $D = \text{diag}(b, c)$ where $b, c \in \mathbb{R}^d$ with $\|b\|_\infty, \|c\|_\infty < 1$.

This model generalizes the one-dimensional setting in Perdomo et al. (2020), where labels follow a binomial distribution with parameter $\frac{1}{2} + x\theta^* + xb\theta$, for $\theta^* \in (0, \frac{1}{2})$ and $b < \frac{1}{2} - \mu$. Focusing on label shifts is natural in regression: it keeps the feature distribution centered and unchanged across deployments despite performative effects, and it can always be enforced through pre-processing.

The performative term $x^\top D\theta$ enforces coordinate-wise effects. This is consistent with previous work (Cyffers et al., 2024; Izzo et al., 2022; Hardt & Mendler-Dünner, 2023) and also close to the model $y = x^\top \theta_{\text{pop}}^* + \mu^\top \theta + w$ studied by Miller et al. (2021), where the performative effect does not depend on x but only on a fixed vector μ . Assuming linearity in θ is reasonable, as performative effects are expected to be moderate to avoid iterations to diverge. Most existing methods impose explicit constraints on the performative effect (Miller et al., 2021), and our setting is no more restrictive: we only require $\|b\|_\infty, \|c\|_\infty < 1$. We set the second half of θ_{pop}^* to zero to represent spurious features, and c captures the corresponding performative effect. This enables us to express correlations between predictive and spurious features via the block structure of the covariance

$$\Sigma = \begin{bmatrix} \Sigma_1 & \Sigma_{12} \\ \Sigma_{12} & \Sigma_2 \end{bmatrix}, \quad (2)$$

where Σ_1 denotes the covariance for the predictive part, Σ_2 the covariance for the spurious part, and Σ_{12} the covariance between the two blocks. Under this setting, RRM corresponds to solving

$$\theta_k = \arg \min_{\theta \in \mathbb{R}^p} \left\{ \frac{1}{2n} \sum_{i=1}^n \ell \left(x_i^{(k-1)}, y_i^{(k-1)}; \theta \right) + \frac{\lambda}{2} \|\theta\|_2^2 \right\}, \quad (3)$$

where $\{(x_i^{(k-1)}, y_i^{(k-1)})\}_{i=1}^n \stackrel{\text{i.i.d.}}{\sim} \mathcal{D}(\theta_{k-1})$ and ℓ is the squared loss. This defines a recurring sequence in both population and over-parameterized regimes. In the population case, the sequence converges in parameter space to a fixed vector θ_{pop}^* (Section 4), while in the over-parameterized case the vector varies at each iteration but the excess risk still converges deterministically (Section 5).

We evaluate the test risk when the final model is deployed on $\mathcal{D}(\theta = 0)$. This ensures that the final model is not evaluated on shifted distributions, and it is particularly relevant for long-term fairness,

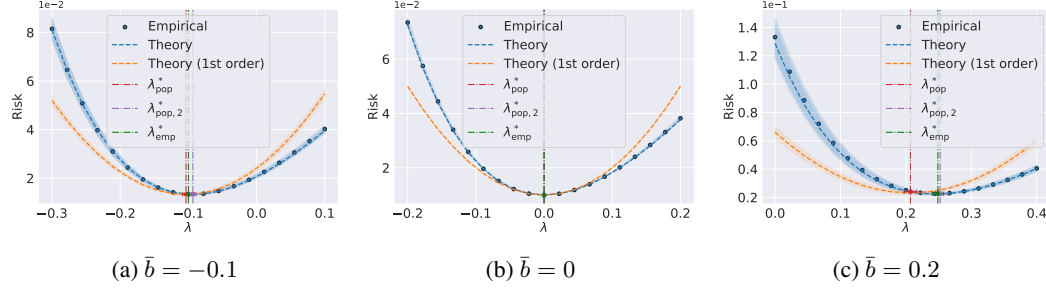


Figure 1: Excess risk at the performative fixed point θ^∞ in (6), as a function of ridge regularization λ , for $d = 100$, $\Sigma = I_p$, entries of b uniform in $[\min\{0, 2\bar{b}\}, \max\{0, 2\bar{b}\}]$, $c = 0$ and $\sigma = 0.1$. Empirical values (blue dots) are computed from 20 i.i.d. trials on a and 5 i.i.d. trials on b , with error band at 1 standard deviation. Theoretical predictions (blue dashed curves) are from (7) and match perfectly empirical values. First-order approximations (orange dashed curves) are given by $\tilde{\mathcal{R}}_{\text{pop}}(D, \lambda, \Sigma)$ in (8) and still provide a good match when λ is near-optimal. The green vertical line is the optimal regularization obtained by numerically optimizing the excess risk of θ^∞ (λ_{emp}^*), the red one is the first-order approximation (λ_{pop}^* from (11)) and the violet one the second-order approximation ($\lambda_{\text{pop},2}^*$ minimizing (12)).

as it prevents bias amplification over time (Ensign et al., 2018; Taori & Hashimoto, 2023) and discourages reliance on spurious features (Bombari & Mondelli, 2025). We thus aim to minimize the following excess risk:

$$\mathcal{R}(\Sigma, \theta, \theta_{\text{pop}}^*) := \mathbb{E}_{\mathcal{D}(\theta=0)} [(y - x^\top \theta)^2] - \sigma^2 = \|\Sigma^{1/2}(\theta - \theta_{\text{pop}}^*)\|_2^2, \quad (4)$$

where we have subtracted the Bayes risk σ^2 . In Section 4, we analyze this risk in the population setting, where enough data is available to exactly recover the parameter vector. Here, the optimal solution is θ_{pop}^* , as suggested by the notation, and testing in-distribution instead of on $\mathcal{D}(\theta = 0)$ trivially yields zero risk, which also motivates the choice of reporting the excess risk on the untouched distribution. In Section 5, we then focus on the over-parameterized regime where $p > n$.

4 ANALYSIS IN THE POPULATION SETTING

In this section, we tackle the population regime where there are enough samples from $\mathcal{D}(\theta_k)$ at each deployment to compute exactly the next regressor, as would typically happen in a low-dimensional setting. The sequence $(\theta_k)_k$ is thus deterministically defined by

$$\theta_k = (\Sigma + \lambda I_p)^{-1} \mathbb{E}_{(x,y) \sim \mathcal{D}(\theta_{k-1})} [xy] = (\Sigma + \lambda I_p)^{-1} (\Sigma \theta_{\text{pop}}^* + \Sigma D \theta_{k-1}), \quad (5)$$

where in the second equality we plug back the definition of the current data distribution in (1).

Excess risk at the performative fixed point. By unrolling (5), we have that the sequence $(\theta_k)_k$ converges at an exponential rate to the fixed point

$$\theta^\infty = (I_p + \lambda \Sigma^{-1} - D)^{-1} \theta_{\text{pop}}^*. \quad (6)$$

The formal statement, including an explicit convergence rate, is deferred to Lemma 5 in Appendix A. By inserting (6) into (4) and taking the expectation with respect to θ_{pop}^* , we have

$$\mathbb{E}_{\theta_{\text{pop}}^*} \mathcal{R}(\Sigma, \theta^\infty, \theta_{\text{pop}}^*) = \mathbb{E}_{\theta_{\text{pop}}^*} [(\theta_{\text{pop}}^*)^\top A^\top \Sigma A \theta_{\text{pop}}^*] = \frac{1}{d} \text{Tr} [(A^\top \Sigma A)_1], \quad (7)$$

where we define $A := (\Sigma + \lambda I_p - \Sigma D)^{-1} \Sigma - I_p$, use $(\theta_{\text{pop}}^*)^\top = (a^\top, 0)$ with a having covariance I_d/d and, given a $p \times p$ matrix M , denote by $(M)_1$ its top-left $d \times d$ block. This leads to the following approximation for the excess risk, also proved in Appendix A.

Theorem 1 (Excess risk – population). *Let $F = D - \lambda \Sigma^{-1}$. Then, we have*

$$\begin{aligned} \mathbb{E}_{\theta_{\text{pop}}^*} \mathcal{R}(\Sigma, \theta^\infty, \theta_{\text{pop}}^*) &= \tilde{\mathcal{R}}_{\text{pop}}(D, \lambda, \Sigma) + O(\|F\|_{\text{op}}^2), \\ \tilde{\mathcal{R}}_{\text{pop}}(D, \lambda, \Sigma) &:= \frac{1}{d} \text{Tr}[\text{diag}(b^2) \Sigma_1] - 2\lambda \bar{b} + \frac{1}{d} \lambda^2 \text{Tr}(S_1), \end{aligned} \quad (8)$$

where $\|\cdot\|_{\text{op}}$ denotes the operator norm, $\bar{b} := \frac{1}{d} \text{Tr}[\text{diag}(b)] = \frac{1}{d} \sum_{i=1}^d b_i$, $b^2 := [b_1^2, \dots, b_d^2] \in \mathbb{R}^d$ and $S_1 = (\Sigma_1 - \Sigma_{12} \Sigma_2^{-1} \Sigma_{21})^{-1}$ denotes the Schur complement of Σ .

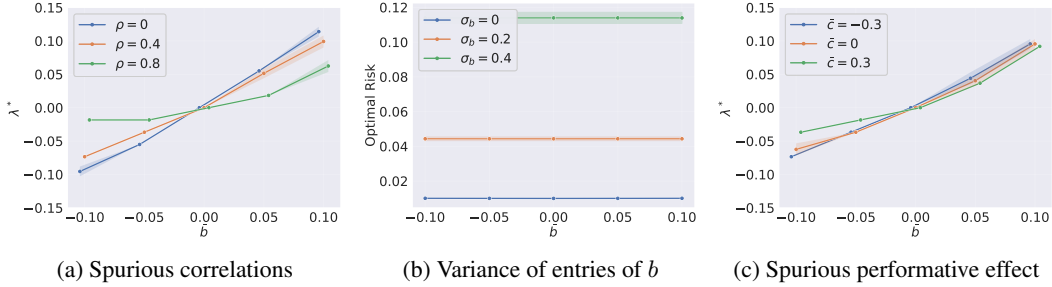


Figure 2: Optimal regularization and risk for the performative fixed point θ^∞ in (6), with $d = 100$, $\Sigma_1 = \Sigma_2 = I_d$, $\Sigma_{12} = \rho I_d$. Values are computed from 20 i.i.d. trials on a and 5 i.i.d. trials on b , with error band at 1 standard deviation. (a) Optimal regularization as a function of \bar{b} for $\rho \in \{0, 0.4, 0.8\}$. The entries of b are uniform in $[\min\{0, 2\bar{b}\}, \max\{0, 2\bar{b}\}]$ and $c = 0$. (b) Optimal risk as a function of \bar{b} . Different curves correspond to different variances σ_b^2 of the entries of b , which are uniform in $[\bar{b} - \sigma_b\sqrt{3}, \bar{b} + \sigma_b\sqrt{3}]$ for $\sigma_b \in \{0, 0.2, 0.4\}$. We pick $c = 0$ and $\rho = 0$. We note that, when $\rho = 0$, $\mathcal{R}_{\text{pop}}^*(D, \Sigma)$ equals the empirical variance of the entries of b and, as such, it does not depend on \bar{b} . (c) Optimal regularization as a function of \bar{b} for $\bar{c} \in \{-0.3, 0, 0.3\}$. The entries of b are uniform in $[\min\{0, 2\bar{b}\}, \max\{0, 2\bar{b}\}]$, the entries of c are uniform in $[\min\{0, 2\bar{c}\}, \max\{0, 2\bar{c}\}]$, and $\rho = 0.5$.

We note that the matrix $F = D - \lambda \Sigma^{-1}$ naturally appears in the computation, and an application of Weyl's inequality (see Lemma 6 in Appendix A) gives

$$\|F\|_{\text{op}} \leq \max \left(\left| \max_{1 \leq i \leq d} \{b_i, c_i\} - \frac{\lambda}{\|\Sigma\|_{\text{op}}} \right|, \left| \min_{1 \leq i \leq d} \{b_i, c_i\} - \frac{\lambda}{\lambda_{\min}(\Sigma)} \right| \right), \quad (9)$$

where $\lambda_{\min}(\Sigma)$ is the smallest eigenvalue of Σ . From (9), we see that the approximation $O(\|F\|_{\text{op}}^2)$ is tighter than $O(\max(\|b\|_\infty, \|c\|_\infty, \lambda)^2)$, since b and c can be partially canceled by λ . In fact, this cancellation occurs when λ is near-optimal, resulting in an accurate approximation, see Figure 1.

Optimal regularization and optimally regularized risk. Leveraging the risk expression for small F of Theorem 1, we next study the behavior of the optimal regularization and of the corresponding optimal risk. More formally, let us define

$$\lambda_{\text{pop}}^*(D, \Sigma) := \arg \min_{\lambda \in \mathbb{R}} \tilde{\mathcal{R}}_{\text{pop}}(D, \lambda, \Sigma), \quad \mathcal{R}_{\text{pop}}^*(D, \Sigma) := \min_{\lambda \in \mathbb{R}} \tilde{\mathcal{R}}_{\text{pop}}(D, \lambda, \Sigma). \quad (10)$$

From (8), we note that $\tilde{\mathcal{R}}_{\text{pop}}(D, \lambda, \Sigma)$ is quadratic in λ , so the minimization in (10) can be readily solved explicitly, leading to the expressions below.

Corollary 2 (Optimal regularization – population). *In the setting described above, we have*

$$\lambda_{\text{pop}}^*(D, \Sigma) = \frac{\bar{b}d}{\text{Tr}(S_1)}, \quad \mathcal{R}_{\text{pop}}^*(D, \Sigma) = \frac{1}{d} \text{Tr}(\text{diag}(b^2) \Sigma_1) - \frac{\bar{b}^2 d}{\text{Tr}(S_1)}. \quad (11)$$

These formulas call for several comments. First, the optimal regularization $\lambda_{\text{pop}}^*(D, \Sigma)$ is proportional to the strength of the performative effect \bar{b} , see Figure 2a (and also the location of the minima in Figure 1). The fact that $\lambda_{\text{pop}}^*(D, \Sigma)$ grows with \bar{b} captures an effect common in practice: when performativity reinforces existing trends —corresponding to “rich-get-richer” phenomena, such as a feature becoming more important over successive deployments—the optimal regularizer increases and helps to limit this effect. Conversely, when the performative effect already mitigates the influence of some feature, the optimal solution calls for less regularization. In the population case, this corresponds to negative regularization (see Figure 1a) which, although less common, has also been studied in the literature (Wu & Xu, 2020; Tsigler & Bartlett, 2023; Patil et al., 2024). Spurious correlations tend to reduce the optimal regularization, although their effect is mild, see Figure 2a.

Second, the optimal risk $\mathcal{R}_{\text{pop}}^*(D, \Sigma)$ is always positive and, thus, worse than in the non-performative scenario, where it is zero. More specifically, zero excess risk can only be reached with a non-zero b if $\Sigma = I_p$ and b is aligned with the all-1 vector, see the blue line in Figure 2b. Intuitively, as regularization impacts all features equally, it better compensates performativity in this uniform case. If the variance in the entries of b grows, then $\mathcal{R}_{\text{pop}}^*(D, \Sigma)$ increases, see Figure 2b.

We finally note that $\tilde{\mathcal{R}}_{\text{pop}}(D, \lambda, \Sigma)$ does not depend on c and, in fact, the effect of c only becomes visible at higher order, as seen in this formula, proven in Section A:

$$\begin{aligned} \mathbb{E}_{\theta^*_{\text{pop}}} \mathcal{R}(\Sigma, \theta^\infty, \theta^*_{\text{pop}}) &= \frac{1}{d} \left(-2\lambda^3 \text{Tr}[(\Sigma^{-2})_1] + \lambda^2 (\text{Tr}[S_1] + 6 \text{Tr}[\text{diag}(b)S_1]) \right. \\ &\quad - \lambda \left(2 \text{Tr}[\text{diag}(b)\Sigma_1 \text{diag}(b)S_1] + 2 \text{Tr}[\text{diag}(b)\Sigma_{12} \text{diag}(c)S_{21}] + 2d\bar{b} + 4 \text{Tr}[\text{diag}(b^2)] \right) \\ &\quad \left. + \text{Tr}[\text{diag}(b^2)\Sigma_1] + 2 \text{Tr}[\text{diag}(b^3)\Sigma_1] \right) + O(\|F\|_{\text{op}}^4), \end{aligned} \quad (12)$$

where $S_{21}^\top = -(\Sigma_1 - \Sigma_{12}\Sigma_2^{-1}\Sigma_{21})^{-1}\Sigma_{12}\Sigma_2^{-1}$ is the off-diagonal precision block. Figure 1 illustrates that the minimizer of this second-order approximation ($\lambda_{\text{pop},2}^*$) is close to the minimizer obtained numerically (λ_{emp}^*). While c tends to steer the optimal regularizer in the opposite direction (less regularization in the case of a self-reinforcing performative effect), it does so only through the cross term $2 \text{Tr}[\text{diag}(b)\Sigma_{12} \text{diag}(c)S_{21}]$, which also depends on b . Figure 2c shows that c moves the optimal regularization in a direction opposite to its sign, but its effect remains rather limited.

5 ANALYSIS IN THE OVER-PARAMETERIZED SETTING

Next, we consider the case where n, p are both large and scale proportionally, with $p/n = \kappa > 1$. All *constants* (e.g., R, M) are intended to be positive values independent of n, p . For mathematical convenience, we opt for a different normalization w.r.t. (3), and the estimator θ_k is given by

$$\theta_k = \arg \min_{\theta \in \mathbb{R}^p} \left\{ \frac{1}{2p} \sum_{i=1}^n \ell(x_i^{(k-1)}, y_i^{(k-1)}; \theta) + \frac{\lambda}{2} \|\theta\|_2^2 \right\}. \quad (13)$$

Solving for θ_k yields

$$\theta_k = \frac{1}{p} \left(\frac{1}{p} X^{(k-1)\top} X^{(k-1)} + \lambda I_p \right)^{-1} X^{(k-1)\top} y^{(k-1)}, \quad (14)$$

where $X^{(k-1)} = [x_1^{(k-1)}, \dots, x_n^{(k-1)}] \in \mathbb{R}^{n \times p}$ and $y^{(k-1)} = [y_1^{(k-1)}, \dots, y_n^{(k-1)}] \in \mathbb{R}^n$. Note that, when θ_k is given by (14), the risk $\mathcal{R}(\Sigma, \theta_k, \theta^*_{\text{pop}})$ as defined in (4) is a random quantity since the data $\{X^{(\ell)}\}_{\ell=1}^{k-1}$ and the noise contained in the labels $\{y^{(\ell)}\}_{\ell=1}^{k-1}$ are random. This makes it challenging to characterize optimal ridge penalty and optimally-tuned risk. To address the challenge, we first establish a *deterministic* equivalent of the risk at the performative fixed point. We next optimize such deterministic equivalent and study the effect of performativity on the optimal regularization.

Deterministic equivalent of the performative fixed point. First, note that, if we regard the performative effect as small and aim at characterizing its effect on the fixed point up to the leading (first) order, it suffices to do two iterations of the recursion in (14). In fact, the labels $y^{(k-1)}$ are linear in $D\theta_{k-1}$, so we expect that, after two iterations, the performative fixed point is reached up to fluctuations of order $O(\|D\|_{\text{op}}^2)$. This is still a random quantity, so we apply techniques from Han & Xu (2023) (and more precisely from Ildiz et al. (2025)) to derive a deterministic equivalent.

Theorem 3 (Excess risk – over-parameterized). *Let $R > 0$ be a constant s.t. $\theta^*_{\text{pop}}, \theta_0 \in B_p(R)$. Assume that $\kappa, \sigma, \lambda \in (1/M, M)$ and $\|\Sigma\|_{\text{op}}, \|\Sigma^{-1}\|_{\text{op}} \leq M$ for some constant $M > 1$. Then, there exists a constant $C = C(M, R)$ such that for any $\delta \in (0, 1/2]$, with probability at least $1 - Cpe^{-p\delta^4/C}$,*

$$|\mathcal{R}(\Sigma, \theta_2, \theta^*_{\text{pop}}) - \mathcal{R}_{\text{eq}}(\Sigma, \theta^*_{\text{pop}}, D, \lambda)| \leq \delta + O(\|D\|_{\text{op}}^2), \quad (15)$$

where

$$\begin{aligned} \mathcal{R}_{\text{eq}}(\Sigma, \theta^*_{\text{pop}}, D, \lambda) &= \tau \langle \theta^*_{\text{pop}}, (\Sigma + \tau I_p)^{-1} (\tau I_p - 2(\Sigma + \tau I_p)^{-1} \Sigma^2 D) \Sigma (\Sigma + \tau I_p)^{-1} \theta^*_{\text{pop}} \rangle \\ &\quad + \kappa \text{Tr} \left[\Sigma^2 (\Sigma + \tau I_p)^{-2} \right] \frac{\sigma^2 + \tau^2 \langle \theta^*_{\text{pop}}, (\Sigma + \tau I_p)^{-1} (I_p + 2(\Sigma + \tau I_p)^{-1} \Sigma D) \Sigma (\Sigma + \tau I_p)^{-1} \theta^*_{\text{pop}} \rangle}{p - \kappa \text{Tr} \left[\Sigma^2 (\Sigma + \tau I_p)^{-2} \right]}, \end{aligned} \quad (16)$$

and τ is the unique solution of

$$\kappa^{-1} - \frac{\lambda}{\tau} = \frac{1}{p} \text{Tr} [(\Sigma + \tau I_p)^{-1} \Sigma]. \quad (17)$$

In words, Theorem 3 shows that the risk $\mathcal{R}(\Sigma, \theta_2, \theta_{\text{pop}}^*)$ is well approximated by the quantity $\widehat{\mathcal{R}}_{\text{eq}}(\Sigma, \theta_{\text{pop}}^*, D, \lambda)$ defined in (16). We highlight that this quantity does not depend on the initialization θ_0 : up a fluctuation of order $O(\|D\|_{\text{op}}^2)$, *the risk has reached a fixed point* after two iterations. While the data—and consequently $\mathcal{R}(\Sigma, \theta_2, \theta_{\text{pop}}^*)$ —are random, $\mathcal{R}_{\text{eq}}(\Sigma, \theta_{\text{pop}}^*, D, \lambda)$ provides a *deterministic equivalent* that depends only on the population covariance Σ , the ground-truth vector θ_{pop}^* , the matrix D capturing the performative effect and the regularization λ .

The assumptions $(\theta_{\text{pop}}^*, \theta_0 \in B_p(R), \kappa, \sigma, \lambda \in (1/M, M), \|\Sigma\|_{\text{op}}, \|\Sigma^{-1}\|_{\text{op}} \leq M)$ are all standard in the related literature (Han & Xu, 2023; Ildiz et al., 2025). We could also handle the ridgeless case $\lambda = 0$ in a similar way to Han & Xu (2023); Ildiz et al. (2025). However, this requires changing some details and we have opted to avoid the notation clutter, since our focus is on the effect of regularization. The proof of Theorem 3 is deferred to Appendix B, and we give a sketch below.

Proof sketch. Having fixed the initialization θ_0 , the only randomness in $\mathcal{R}(\Sigma, \theta_1, \theta_{\text{pop}}^*)$ comes from $(X^{(0)}, y^{(0)})$. This corresponds to the setting in which one trains using the vector of regression coefficients $\theta_{\text{pop}}^* + D\theta_0$ and then tests on θ_{pop}^* . Lemma 7 in Appendix B (which follows from Theorem 3 by Ildiz et al. (2025) and uses the non-asymptotic characterization of the minimum norm interpolator by Han & Xu (2023)) gives that, with high probability, $\mathcal{R}(\Sigma, \theta_1, \theta_{\text{pop}}^*)$ is close to

$$\begin{aligned} \mathcal{R}_{\text{eq}}^{(1)}(\Sigma, \theta_0, \theta_{\text{pop}}^*) &= \left\| (\Sigma + \tau I_p)^{-1} \Sigma (\theta_{\text{pop}}^* + D\theta_0) - \theta_{\text{pop}}^* \right\|_{\Sigma}^2 \\ &+ \kappa \text{Tr} \left[\Sigma^2 (\Sigma + \tau I_p)^{-2} \right] \frac{\sigma^2 + \tau^2 \left\| (\Sigma + \tau I_p)^{-1} (\theta_{\text{pop}}^* + D\theta_0) \right\|_{\Sigma}^2}{p - \kappa \text{Tr} \left[\Sigma^2 (\Sigma + \tau I_p)^{-2} \right]}, \end{aligned} \quad (18)$$

where $\|x\|_{\Sigma}^2 := x^{\top} \Sigma x$. We note that the expression in (18) depends on θ_0 and, in fact, it keeps depending on it even after neglecting terms of order $O(\|D\|_{\text{op}}^2)$. This means that we have not yet reached the fixed point. Thus, we turn our attention to the risk after two iterations and, by iterating twice the strategy of Lemma 7, we show that, with high probability, $\mathcal{R}(\Sigma, \theta_2, \theta_{\text{pop}}^*)$ is close to $\mathcal{R}_{\text{eq}}^{(2)}(\Sigma, \theta_0, \theta_{\text{pop}}^*)$, whose expression is given in Lemma 8 in Appendix B. Finally, by neglecting terms of order $O(\|D_{\text{op}}\|^2)$ in $\mathcal{R}_{\text{eq}}^{(2)}(\Sigma, \theta_0, \theta_{\text{pop}}^*)$, this quantity equals $\mathcal{R}_{\text{eq}}(\Sigma, \theta_{\text{pop}}^*, D, \lambda)$ in (16), and the desired result follows. \square

Optimal regularization and optimally regularized risk. Leveraging the characterization of Theorem 3, we optimize the ridge regularization. We focus on the case $\Sigma = \begin{bmatrix} I_d & \rho I_d \\ \rho I_d & I_d \end{bmatrix}$ for small ρ . While simplified, this setting captures the performative effect of both predictive and spurious features, leading to an interesting phenomenology. Lemma 9 in Appendix C computes $\mathbb{E}_{\theta_{\text{pop}}^*} \mathcal{R}_{\text{eq}}(\Sigma, \theta_{\text{pop}}^*, D, \lambda)$, as well as the following expansion in ρ :

$$\begin{aligned} \mathbb{E}_{\theta_{\text{pop}}^*} \mathcal{R}_{\text{eq}}(\Sigma, \theta_{\text{pop}}^*, D, \lambda) &= \widetilde{\mathcal{R}}(D, \lambda, \rho) + O(\bar{b}\rho^2 + \rho^4), \\ \widetilde{\mathcal{R}}(D, \lambda, \rho) &:= \mathcal{R}_0(\lambda, \rho) + \bar{b}A_1(\lambda) + \bar{c}\rho^2 A_2(\lambda), \end{aligned} \quad (19)$$

with $\bar{b} = \text{Tr}[\text{diag}(b)]/d$, $\bar{c} = \text{Tr}[\text{diag}(c)]/d$. Explicit expressions for $\mathcal{R}_0(\lambda, \rho)$, $A_1(\lambda)$ and $A_2(\lambda)$ are given in (46) in Appendix C. We note that $\mathbb{E}_{\theta_{\text{pop}}^*} \mathcal{R}_{\text{eq}}(\Sigma, \theta_{\text{pop}}^*, D, \lambda)$ is even in ρ , hence the odd powers of ρ are absent from (19). Now, we define optimal regularization and risk as

$$\lambda_{\text{eq}}^*(D, \rho) := \arg \min_{\lambda \geq 0} \widetilde{\mathcal{R}}(D, \lambda, \rho), \quad \mathcal{R}_{\text{eq}}^*(D, \rho) := \min_{\lambda \geq 0} \widetilde{\mathcal{R}}(D, \lambda, \rho). \quad (20)$$

Our goal is to characterize the performative effect on $\lambda_{\text{eq}}^*(D, \lambda, \rho)$, $\mathcal{R}_{\text{eq}}^*(D, \lambda, \rho)$ and, to do so, we compare these quantities to their values when $D = 0$, defined as

$$\lambda_{\text{eq}, D=0}^*(\rho) := \arg \min_{\lambda \geq 0} \mathcal{R}_0(\lambda, \rho), \quad \mathcal{R}_{\text{eq}}^*(\rho) = \min_{\lambda \geq 0} \mathcal{R}_0(\lambda, \rho). \quad (21)$$

This is formalized by the result below whose proof is deferred to Appendix C.

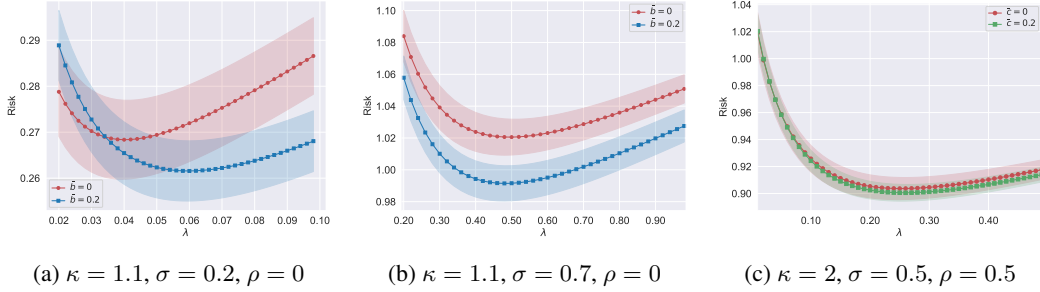


Figure 3: Excess risk as a function of ridge regularization λ with Gaussian data, for $n = 4000$, $\Sigma_1 = \Sigma_2 = I_d$, $\Sigma_{12} = \rho I_d$, entries of b equal to \bar{b} , and entries of c equal to \bar{c} . Values are computed from 20 i.i.d. trials, with error band at 1 standard deviation. We perform 5 steps of RRM to approximate the fixed point, as in the simulation setup of Section 6. (a) In the low-noise regime ($\sigma = 0.2$), taking $\bar{b} = 0.2$ instead of $\bar{b} = 0$ *increases the optimal regularization and reduces the optimal risk*. We set $\bar{c} = 0$ to emphasize the dependence on \bar{b} . (b) In the large-noise regime ($\sigma = 0.7$), taking $\bar{b} = 0.2$ instead of $\bar{b} = 0$ *reduces both optimal regularization and optimal risk*. As in (a), we set $\bar{c} = 0$. (c) Taking $\bar{c} = 0.2$ instead of $\bar{c} = 0$ *reduces the optimal risk*, although the the impact of \bar{c} is less pronounced. We set $\bar{b} = 0$ to emphasize the dependence on \bar{c} .

Theorem 4 (Optimal regularization – over-parameterized). *In the setting described above, we have*

$$\lambda_{\text{eq}}^*(D, \rho) = \lambda_{\text{eq}, D=0}^*(\rho) + \bar{b}(B_1(\sigma, \kappa) + O(\rho^2)) + \bar{c}\rho^2(C_1(\sigma, \kappa) + O(\rho^2)) + O(\bar{b}^2 + \bar{c}^2), \quad (22)$$

$$\mathcal{R}_{\text{eq}}^*(D, \rho) = \mathcal{R}_{\text{eq}}^*(\rho) + \bar{b}(B_2(\sigma, \kappa) + O(\rho^2)) + \bar{c}\rho^2(C_2(\sigma, \kappa) + O(\rho^2)) + O(\bar{b}^2 + \bar{c}^2), \quad (23)$$

where the functions $B_1(\sigma, \kappa)$, $B_2(\sigma, \kappa)$, $C_1(\sigma, \kappa)$, $C_2(\sigma, \kappa)$ depend only on σ, κ and they are explicitly given in (51)-(53). Furthermore, these functions satisfy

$$B_1(\sigma, \kappa) \geq 0 \quad \text{for } 0 \leq \sigma \leq \sigma_{B_1}(\kappa), \kappa > 1, \quad B_1(\sigma, \kappa) \leq 0 \quad \text{for } \sigma > \sigma_{B_1}(\kappa), \kappa > 1, \quad (24)$$

$$C_1(\kappa, \sigma) \leq 0 \quad \text{for } \sigma \geq 0, \kappa \geq 2, \quad (25)$$

$$B_2(\kappa, \sigma) \leq 0 \quad \text{for } \sigma \geq 0, \kappa > 1, \quad (26)$$

$$C_2(\kappa, \sigma) \leq 0 \quad \text{for } \sigma \geq 0, \kappa > 1, \quad (27)$$

with $\sigma_{B_1}^2(\kappa) = 1/2 - 7\kappa^{-1}/18 + O(\kappa^{-2})$.

In words, (22) gives a quantitative comparison between optimal regularization with performativity effect ($\lambda_{\text{eq}}^*(D, \rho)$) and without it ($\lambda_{\text{eq}, D=0}^*(\rho)$). Similarly, (23) compares optimally-regularized risks $\mathcal{R}_{\text{eq}}^*(D, \rho)$ and $\mathcal{R}_{\text{eq}}^*(\rho)$ respectively with and without performativity. The study of the signs of the auxiliary functions $B_1(\sigma, \kappa)$, $B_2(\sigma, \kappa)$, $C_1(\sigma, \kappa)$, $C_2(\sigma, \kappa)$ leads to the considerations below:

- Equation (24) implies that (i) if the noise variance σ^2 is small, then the optimal regularization moves in the same direction as the performativity effect on the predictive features; and (ii) if the noise variance is large, the effect is reversed and the optimal regularization moves in the opposite direction to the performativity effect. This is illustrated in Figures 3a and 3b.
- Equation (25) implies that, when $\kappa \geq 2$, the optimal regularization moves in the opposite direction to the performativity effect on the spurious features. This effect is however significantly attenuated by the factor ρ^2 multiplying \bar{c} in (22) and, as such, it is hardly noticeable both with Gaussian data (as considered in this section) and in real-world settings (as considered in Section 6).
- Equation (26) implies that, when performativity reinforces existing trends ($\bar{b} > 0$), the optimally-regularized risk improves in the presence of a performativity effect on the predictive features. This occurs regardless of the size of the noise variance, and it is illustrated in Figures 3a and 3b. Instead, when performativity dampens existing trends ($\bar{b} < 0$), the effect is reversed and the optimal risk worsens.
- Finally, Equation (27) implies that the dependence of the optimally-regularized risk on the performativity effect on the spurious features is analogous: the optimal risk decreases when $\bar{c} > 0$, and increases when $\bar{c} < 0$. However, as for $\lambda_{\text{eq}}^*(D, \rho)$, the impact of performativity on $\mathcal{R}_{\text{eq}}^*(D, \rho)$ is less pronounced for the spurious features, due to the factor ρ^2 multiplying \bar{c} in (23). This is illustrated in Figure 3c.

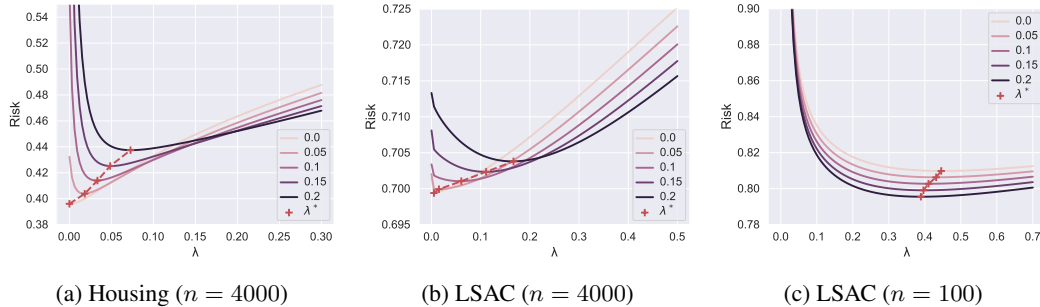


Figure 4: Excess risk as a function of ridge regularization λ in real-world datasets (Housing, LSAC). Different curves (in different colors) correspond to different values of $\bar{b} \in \{0, 0.05, 0.1, 0.15, 0.2\}$, and we connect with a red dashed line the optima of the risk for various choices of \bar{b} . The plots in (a)-(b) use $n = 4000$ data points at each training step, which corresponds to the population setting ($n \gg d$); the plot in (c) uses $n = 100$, a value closer to the number of features $d = 22$.

6 NUMERICAL EXPERIMENTS

In this section, we test the effect of regularization and performative shifts on real data. Since no dataset currently provides a real performative shift, it must be encoded synthetically. In practice, we take a real-world dataset, randomly split the samples across time steps, train a model on one split, compute the parameter θ , and then shift the samples of the next split according to the theoretical model. This methodology follows previous work (Perdomo et al., 2020; Hardt & Mendler-Dünner, 2023; Zezulka & Genin, 2023). These experiments allow us to test whether the theory remains predictive when (i) the data is non-Gaussian and θ_{pop}^* is fixed by the task, and (ii) the true relationship between the feature and the target is likely to not be linear.

We consider two datasets. First, we use the Housing dataset,¹ where the goal is to predict house prices from housing features and local demographics. We follow the methodology of Cyffers et al. (2024) to choose performative features. The dataset has 8 features and 20,640 datapoints, which we split into five folds: four for training and one for test. Four training steps suffice experimentally to reach the fixed point, which is consistent with the theory, where the first-order effect stabilizes after only two iterations. Second, we use the Law School Admission Council (LSAC) dataset,² where the default task is to predict bar passage from demographic features and previous grades. We change the target to GPA to maintain a regression task, and randomly choose which features are affected by performativity. After dropping redundant columns or those too correlated with GPA, the dataset has 22 features and 20,427 samples, which again we split in five folds. We report detailed pre-processing and parameters in Section D.

When $n = 4000$, both for the Housing (Figure 4a) and the LSAC (Figure 4b) dataset, we note that (i) the optimal regularizer increases proportionally to \bar{b} , and (ii) the optimally-regularized risk becomes worse as \bar{b} grows. This can be attributed to the fact that $n \gg d$, and it is consistent with our theoretical results in the population setting (Corollary 2). In contrast, when training with very few samples on LSAC (Figure 4c), the behavior of the regularized risk follows the predictions of Theorem 3 for the proportional setting in the large-noise regime: as \bar{b} grows, the optimal regularizer gets smaller and the risk improves. Note that, even if Figures 4b and 4c consider the same dataset, the ranges of the excess risk and the regularizer are not the same due to the different sample sizes. We did not find numerical evidence for the role of c , suggesting that its effect may be dominated by data noise, consistent with our theoretical findings on the limited impact of spurious features.

7 CONCLUSIONS

In this work, we demonstrate that regularization and performative effect are strongly related, as one can partially cancel out the other. In the population regime, the excess risk is worsened by performative effects. However, optimal ridge regularization mitigates this issue, especially when

¹<https://www.openml.org/d/823>

²https://storage.googleapis.com/lawschool_dataset/bar_pass_prediction.csv

the data is isotropic and the entries of the vector modeling performativity have little variability. In the proportional regime, we provide a deterministic equivalent of the performative fixed point for random data. This in turn unveils a remarkable phenomenology: in contrast with the population setting, the optimal risk improves when performativity reinforces existing trends; furthermore, the optimal regularization follows the direction of the performative effect on the predictive features when the noise is small, while it goes in the opposite direction when the noise is large. Although the theoretical results focus on Gaussian features and a linear target model, our experiments on real-world data follow the theoretical predictions, suggesting their generality. Overall, these findings indicate that regularization could help in a wider range of scenarios, which we leave for future work. Beyond studying more complex data or models, interesting directions include the impact of other forms of regularization, such as early stopping or pruning, to mitigate performative effects.

REPRODUCIBILITY STATEMENT

Additional implementation details are provided in Section D. The code is available at <https://github.com/totillas/regularization-vs-perf>.

ACKNOWLEDGMENTS

This research was funded in whole or in part by the Austrian Science Fund (FWF) 10.55776/COE12. For the purpose of open access, the authors have applied a CC BY public copyright license to any Author Accepted Manuscript version arising from this submission. Alireza Mirrokni was an intern at ISTA while working on this project.

REFERENCES

Peter L. Bartlett, Philip M. Long, Gábor Lugosi, and Alexander Tsigler. Benign overfitting in linear regression. *Proceedings of the National Academy of Sciences*, 117(48), 2020.

Yahav Bechavod, Katrina Ligett, Steven Wu, and Juba Ziani. Gaming helps! learning from strategic interactions in natural dynamics. In *Conference on Uncertainty in Artificial Intelligence (AISTATS)*, volume 130, 2021.

Mikhail Belkin, Daniel Hsu, Siyuan Ma, and Soumik Mandal. Reconciling modern machine-learning practice and the classical bias–variance trade-off. *Proceedings of the National Academy of Sciences*, 116(32), 2019.

Omri Ben-Dov, Jake Fawkes, Samira Samadi, and Amartya Sanyal. The role of learning algorithms in collective action. In *International Conference on Machine Learning (ICML)*, volume 235, 2024.

Simone Bombari and Marco Mondelli. Spurious correlations in high dimensional regression: The roles of regularization, simplicity bias and over-parameterization. In *International Conference on Machine Learning (ICML)*, 2025.

Xiangyu Chang, Yingcong Li, Samet Oymak, and Christos Thrampoulidis. Provable benefits of overparameterization in model compression: From double descent to pruning neural networks. In *Conference on Artificial Intelligence (AAAI)*, volume 35, 2021.

Chen Cheng and Andrea Montanari. Dimension free ridge regression. *The Annals of Statistics*, 52(6), 2024.

Edwige Cyffers, Muni Sreenivas Pydi, Jamal Atif, and Oliver Cappé. Optimal classification under performative distribution shift. In *Conference on Neural Information Processing Systems (NeurIPS)*, volume 37, 2024.

Zeyu Deng, Abla Kammoun, and Christos Thrampoulidis. A model of double descent for high-dimensional binary linear classification. *Information and Inference: A Journal of the IMA*, 11(2), 2022.

Dmitriy Drusvyatskiy and Lin Xiao. Stochastic optimization with decision-dependent distributions. *Mathematics of Operations Research*, 48(2), May 2023.

Danielle Ensign, Sorelle A. Friedler, Scott Neville, Carlos Scheidegger, and Suresh Venkatasubramanian. Runaway feedback loops in predictive policing. In *Conference on Fairness, Accountability and Transparency (FAccT)*, volume 81, 2018.

Alhussein Fawzi, Omar Fawzi, and Pascal Frossard. Analysis of classifiers' robustness to adversarial perturbations. *Machine learning*, 107(3):481–508, 2018.

Qiyang Han and Xiaocong Xu. The distribution of ridgeless least squares interpolators. *arXiv preprint arXiv:2307.02044*, 2023.

Moritz Hardt and Celestine Mendler-Dünner. Performative prediction: Past and future. *arXiv preprint arXiv:2310.16608*, 2023.

Trevor Hastie, Andrea Montanari, Saharon Rosset, and Ryan J Tibshirani. Surprises in high-dimensional ridgeless least squares interpolation. *Annals of statistics*, 50(2), 2022.

Muhammed Emrullah Ildiz, Halil Alperen Gozeten, Ege Onur Taga, Marco Mondelli, and Samet Oymak. High-dimensional analysis of knowledge distillation: Weak-to-strong generalization and scaling laws. In *International Conference on Learning Representations (ICLR)*, 2025.

Zachary Izzo, James Zou, and Lexing Ying. How to learn when data gradually reacts to your model. In *Conference on Uncertainty in Artificial Intelligence (AISTATS)*, volume 151, 2022.

Ayush Jain, Andrea Montanari, and Eren Sasoglu. Scaling laws for learning with real and surrogate data. In *Conference on Neural Information Processing Systems (NeurIPS)*, volume 37, 2024.

Germain Kolossov, Andrea Montanari, and Pulkit Tandon. Towards a statistical theory of data selection under weak supervision. In *International Conference on Learning Representations (ICLR)*, 2024.

Qiang Li, Chung-Yiu Yau, and Hoi-To Wai. Multi-agent performative prediction with greedy deployment and consensus seeking agents. In *Conference on Neural Information Processing Systems (NeurIPS)*, volume 35, 2022.

Neil Rohit Mallinar, Austin Zane, Spencer Frei, and Bin Yu. Minimum-norm interpolation under covariate shift. In *International Conference on Machine Learning (ICML)*, volume 235, 2024.

John Miller, Juan C. Perdomo, and Tijana Zrnic. Outside the echo chamber: Optimizing the performative risk. In *International Conference on Machine Learning (ICML)*, volume 139, 2021.

Andrea Montanari, Feng Ruan, Youngtak Sohn, and Jun Yan. The generalization error of max-margin linear classifiers: Benign overfitting and high dimensional asymptotics in the overparametrized regime. *Annals of statistics*, 53(2), 2025.

Oskar Morgenstern. *Wirtschaftsprägnose: Eine Untersuchung ihrer Voraussetzungen und Möglichkeiten*. Springer, 1928. ISBN 978-3709121139.

Adhyyan Narang, Evan Faulkner, Dmitriy Drusvyatskiy, Maryam Fazel, and Lillian J. Ratliff. Multiplayer performative prediction: Learning in decision-dependent games. *Journal of Machine Learning Research*, 24(202), 2023.

Alexander Pan, Erik Jones, Meena Jagadeesan, and Jacob Steinhardt. Feedback loops with language models drive in-context reward hacking. In *International Conference on Machine Learning (ICML)*, volume 235, 2024.

Pratik Patil, Jin-Hong Du, and Ryan J Tibshirani. Optimal ridge regularization for out-of-distribution prediction. In *International Conference on Machine Learning (ICML)*, volume 235, 2024.

Juan Perdomo, Tijana Zrnic, Celestine Mendler-Dünner, and Moritz Hardt. Performative prediction. In *International Conference on Machine Learning (ICML)*, volume 119, 2020.

Antonio H. Ribeiro, Dave Zachariah, Francis Bach, and Thomas B. Schön. Regularization properties of adversarially-trained linear regression. In *Conference on Neural Information Processing Systems (NeurIPS)*, volume 36, 2023.

Dominic Richards, Jaouad Mourtada, and Lorenzo Rosasco. Asymptotics of ridge (less) regression under general source condition. In *Conference on Uncertainty in Artificial Intelligence (AISTATS)*, volume 130, 2021.

Yanke Song, Sohom Bhattacharya, and Pragya Sur. Generalization error of min-norm interpolators in transfer learning. *arXiv preprint arXiv:2406.13944*, 2024.

Rohan Taori and Tatsunori Hashimoto. Data feedback loops: Model-driven amplification of dataset biases. In *International Conference on Machine Learning (ICML)*, volume 202, 2023.

Alexander Tsigler and Peter L Bartlett. Benign overfitting in ridge regression. *Journal of Machine Learning Research*, 24(123), 2023.

Raluca Mihaela Ursu. The power of rankings: Quantifying the effects of rankings on online consumer search and choice. *SSRN Electronic Journal*, 2015.

Xiaolu Wang, Chung-Yiu Yau, and Hoi To Wai. Network effects in performative prediction games. In *International Conference on Machine Learning (ICML)*, volume 202, 2023.

Denny Wu and Ji Xu. On the optimal weighted ℓ_2 regularization in overparameterized linear regression. In *Conference on Neural Information Processing Systems (NeurIPS)*, volume 33, 2020.

Fan Yang, Hongyang R Zhang, Sen Wu, Christopher Re, and Weijie J Su. Precise high-dimensional asymptotics for quantifying heterogeneous transfers. *Journal of Machine Learning Research*, 26(113), 2025.

Sebastian Zezulka and Konstantin Genin. Performativity and Prospective Fairness. *arXiv preprint arXiv:2310.08349*, 2023.

A ADDITIONAL PROOFS FOR SECTION 4

This appendix contains the missing proofs for Section 4. We start with the convergence at exponential rate to the fixed point θ^∞ in (6). Then, we prove Theorem 1 giving the first-order approximation of the risk, as well as the expression in (12) giving the higher-order approximation of the risk. Finally, we prove the upper bound on $\|F\|_{\text{op}}$ in (9).

Lemma 5. *The sequence $(\theta_k)_k$ converges to the fixed point*

$$\theta^\infty = (\Sigma + \lambda I_p - M)^{-1} \Sigma \theta_{\text{pop}}^*.$$

Moreover, for any $\varepsilon \in (0, 1)$, if we start at $\theta_0 = 0$, after at most

$$k_\varepsilon = \left\lceil \frac{\ln(1/\varepsilon)}{\ln\left(1/\left(\frac{\|\Sigma\|_{\text{op}}}{\|\Sigma\|_{\text{op}} + \lambda} \max\{\|b\|_\infty, \|c\|_\infty\}\right)\right)} \right\rceil$$

iterations, the relative error $\frac{\|\theta^{k_\varepsilon} - \theta^\infty\|_2}{\|\theta^\infty\|_2}$ is smaller than ε .

Proof. Denoting $T = (\Sigma + \lambda I_p)^{-1} \Sigma D$, the recurrence relation is

$$\theta^k = T\theta^{k-1} + (\Sigma + \lambda I_p)^{-1} \Sigma \theta_{\text{pop}}^*.$$

When going to the limit, $\sum_i T^i \rightarrow (I_p - T)^{-1}$. The convergence requires the matrix T to have smaller eigenvalues than one, which is guaranteed by $\|b\|_\infty$ and $\|c\|_\infty$ being smaller than 1. Thus, we have

$$\theta^\infty = (I_p - T)^{-1} (\Sigma + \lambda I_p)^{-1} \Sigma \theta_{\text{pop}}^*.$$

Noticing that $I_p = (\Sigma + \lambda I_p)^{-1} (\Sigma + \lambda I_p)$ and using the definition of T gives the expression of θ_∞ .

Let $e_k = \theta^k - \theta^\infty$. Using $\theta^\infty = T\theta^\infty + (\Sigma + \lambda I_p)^{-1} \Sigma \theta_{\text{pop}}^*$, we have

$$e_k = \theta^k - \theta^\infty = T\theta^{k-1} + (\Sigma + \lambda I_p)^{-1} \Sigma \theta_{\text{pop}}^* - \theta^\infty = T(\theta^{k-1} - \theta^\infty) = T e_{k-1}.$$

Thus,

$$e_k = T^k e_0 = -T^k \theta^\infty \implies \|e_k\|_2 \leq \|T\|_{\text{op}}^k \|\theta^\infty\|_2 \implies \frac{\|e_k\|_2}{\|\theta^\infty\|_2} = \frac{\|\theta^k - \theta^\infty\|_2}{\|\theta^\infty\|_2} \leq \|T\|_{\text{op}}^k.$$

Consequently, $\|T\|^k \leq \varepsilon$ suffices, i.e., $k \geq \ln(1/\varepsilon) / \ln(1/\|T\|_{\text{op}})$. We finally note that

$$\|T\|_{\text{op}} \leq \|(\Sigma + \lambda I_p)^{-1} \Sigma\|_{\text{op}} \|D\|_{\text{op}} = \frac{\|\Sigma\|_{\text{op}}}{\|\Sigma\|_{\text{op}} + \lambda} \max\{\|b\|_\infty, \|c\|_\infty\}.$$

Combining the last two inequalities gives the wanted convergence rate. \square

Proof of Theorem 1 and of the higher-order approximation in (12). We start by computing the Taylor expansion:

$$A = (\Sigma + \lambda I_p - \Sigma D)^{-1} \Sigma - I_p = (I_p - (D - \lambda \Sigma^{-1}))^{-1} - I_p = \sum_{i=1}^{\infty} (D - \lambda \Sigma^{-1})^i = \sum_{i=1}^{\infty} F^i.$$

Let us define $A^{(k)} = \sum_{i=1}^k (D - \lambda \Sigma^{-1})^i$. For the two first orders, we have:

$$A^{(1) \top} \Sigma A^{(1)} = (D - \lambda \Sigma^{-1}) \Sigma (D - \lambda \Sigma^{-1}) = D \Sigma D - 2\lambda D + \lambda^2 \Sigma^{-1}.$$

This is independent of c and gives the simple formula

$$R^{(1)}(\lambda) = \frac{1}{d} \text{Tr}(\text{diag}(b^2) \Sigma_1) - 2\lambda \bar{b} + \frac{1}{d} \lambda^2 \text{Tr}(S_1),$$

where $\bar{b} := \frac{1}{d} \text{Tr}[\text{diag}(b)] = \frac{1}{d} \sum_{i=1}^d b_i$, $b^2 := [b_1^2, \dots, b_d^2] \in \mathbb{R}^d$ and $S_1 = (\Sigma_1 - \Sigma_{12}\Sigma_2^{-1}\Sigma_{21})^{-1}$ denotes the Schur complement of Σ . We go further in the expansion to recover (12):

$$\begin{aligned} A^{(2)\top} \Sigma A^{(2)} &= A^{(1)\top} \Sigma A^{(1)} + A^{(1)\top} \Sigma \left(A^{(2)} - A^{(1)} \right) + \left(A^{(2)} - A^{(1)} \right)^\top \Sigma A^{(1)} \\ &\quad + \underbrace{\left(A^{(2)} - A^{(1)} \right)^\top \Sigma \left(A^{(2)} - A^{(1)} \right)}_{O(\|F\|_{\text{op}}^4), \text{ discarded}} \\ &= D\Sigma D + D^2\Sigma D + D\Sigma D^2 - \lambda [D\Sigma D\Sigma^{-1} + \Sigma^{-1}D\Sigma D + 2D + 4D^2] \\ &\quad + \lambda^2 [\Sigma^{-1} + 3(\Sigma^{-1}D + D\Sigma^{-1})] - 2\lambda^3\Sigma^{-2} + O(\|F\|_{\text{op}}^4). \end{aligned}$$

The final formula results from taking the trace of the first block. We write the matrix product block per block to prove that

$$\text{Tr}[(D\Sigma D\Sigma^{-1} + \Sigma^{-1}D\Sigma D)_1] = 2\text{Tr}[\text{diag}(b)\Sigma_1 \text{diag}(b)S_1] + 2\text{Tr}[\text{diag}(b)\Sigma_{12} \text{diag}(c)S_{21}],$$

where $S_{21}^\top = -(\Sigma_1 - \Sigma_{12}\Sigma_2^{-1}\Sigma_{21})^{-1}\Sigma_{12}\Sigma_2^{-1}$. This concludes the proof. \square

Lemma 6. *Let $F = D - \lambda\Sigma^{-1}$. Then, we have that*

$$\|F\|_{\text{op}} \leq \max \left(\left| \max_{1 \leq i \leq d} \{b_i, c_i\} - \frac{\lambda}{\lambda_{\max}(\Sigma)} \right|, \left| \min_{1 \leq i \leq d} \{b_i, c_i\} - \frac{\lambda}{\lambda_{\min}(\Sigma)} \right| \right). \quad (28)$$

Proof. By Weyl's inequalities for Hermitian matrices,

$$\begin{aligned} \lambda_{\max}(F) &\leq \lambda_{\max}(D) - \lambda\lambda_{\min}(\Sigma^{-1}) = \max_{1 \leq i \leq d} \{b_i, c_i\} - \frac{\lambda}{\lambda_{\max}(\Sigma)}, \\ \lambda_{\min}(F) &\geq \lambda_{\min}(D) - \lambda\lambda_{\max}(\Sigma^{-1}) = \min_{1 \leq i \leq d} \{b_i, c_i\} - \frac{\lambda}{\lambda_{\min}(\Sigma)}. \end{aligned}$$

Therefore, we have

$$\begin{aligned} \|F\|_{\text{op}} &= \max \{|\lambda_{\max}(F)|, |\lambda_{\min}(F)|\} \\ &\leq \max \left(\left| \max_{1 \leq i \leq d} \{b_i, c_i\} - \frac{\lambda}{\lambda_{\max}(\Sigma)} \right|, \left| \min_{1 \leq i \leq d} \{b_i, c_i\} - \frac{\lambda}{\lambda_{\min}(\Sigma)} \right| \right), \end{aligned}$$

and the equality happens if and only if and only if Σ and D are simultaneously diagonalizable. \square

We finally note that (28) coincides with (9) since $\lambda_{\max}(\Sigma) = \|\Sigma\|_{\text{op}}$, due to Σ being a covariance matrix and, hence, positive semidefinite.

B PROOF OF THEOREM 3

Deterministic equivalent for $\mathcal{R}_1(\Sigma, \theta_1, \theta_{\text{pop}}^*)$. Let $\mathcal{R}_k(\Sigma, \theta_k, \theta_{\text{pop}}^*)$ be the excess risk of the estimator θ_k given by (14), i.e.,

$$\mathcal{R}_k(\Sigma, \theta_k, \theta_{\text{pop}}^*) = \|\theta_k - \theta_{\text{pop}}^*\|_\Sigma^2.$$

Having fixed the initialization θ_0 , the only randomness in $\mathcal{R}_1(\Sigma, \theta_1, \theta_{\text{pop}}^*)$ comes from $(X^{(0)}, y^{(0)})$. This corresponds to the setting in which one trains from the (deterministic) vector of regression coefficients $\theta_{\text{pop}}^* + D\theta_0$. The following lemma gives a deterministic equivalent for $\mathcal{R}_1(\Sigma, \theta_1, \theta_{\text{pop}}^*)$, conditional on θ_0 .

Lemma 7. *Let $R > 0$ be a constant such that $\theta_{\text{pop}}^*, \theta_0 \in B_p(R)$. Assume that $\kappa, \sigma, \lambda \in (1/M, M)$ and $\|\Sigma\|_{\text{op}}, \|\Sigma^{-1}\|_{\text{op}} \leq M$ for some constant $M > 1$. Then, there exists a constant $C = C(M, R)$ such that, for any $\delta \in (0, 1/2]$, the following holds*

$$\sup_{\theta_{\text{pop}}^*, \theta_0 \in B_p(R)} \Pr \left(\left| \mathcal{R}_1(\Sigma, \theta_1, \theta_{\text{pop}}^*) - \mathcal{R}_{\text{eq}}^{(1)}(\Sigma, \theta_0, \theta_{\text{pop}}^*) \right| \geq \delta \right) \leq C p e^{-p\delta^4/C}, \quad (29)$$

where

$$\begin{aligned} \mathcal{R}_{\text{eq}}^{(1)}(\Sigma, \theta_0, \theta_{\text{pop}}^*) &= \left\| (\Sigma + \tau I_p)^{-1} \Sigma (\theta_{\text{pop}}^* + D\theta_0) - \theta_{\text{pop}}^* \right\|_{\Sigma}^2 \\ &+ \kappa \text{Tr} \left[\Sigma^2 (\Sigma + \tau I_p)^{-2} \right] \frac{\sigma^2 + \tau^2 \left\| (\Sigma + \tau I_p)^{-1} (\theta_{\text{pop}}^* + D\theta_0) \right\|_{\Sigma}^2}{p - \kappa \text{Tr} \left[\Sigma^2 (\Sigma + \tau I_p)^{-2} \right]}, \end{aligned} \quad (30)$$

and τ is the unique solution of (17).

Proof. Note that we are generating labels using $\theta_0^{\text{perfo}} := \theta_{\text{pop}}^* + D\theta_0$ as a vector of regression coefficients. Thus, we can apply Theorem 3 by Ildiz et al. (2025) (which utilizes the non-asymptotic characterization of the minimum norm interpolator by Han & Xu (2023)), replacing β^s with θ_0^{perfo} in that statement. This gives that (29) holds with $\mathcal{R}_{\text{eq}}^{(1)}(\Sigma, \theta_0, \theta_{\text{pop}}^*)$ replaced by $\tilde{\mathcal{R}}_{\text{eq}}^{(1)}(\Sigma, \theta_{\text{pop}}^*, \theta_0^{\text{perfo}})$ defined as

$$\tilde{\mathcal{R}}_{\text{eq}}^{(1)}(\Sigma, \theta_{\text{pop}}^*, \theta_0^{\text{perfo}}) = \mathbb{E}_{g^{(1)}} \left[\left\| X^{(1)}(\Sigma, \theta_0^{\text{perfo}}, g^{(1)}) - \theta_{\text{pop}}^* \right\|_{\Sigma}^2 \right], \quad (31)$$

where

$$X^{(1)}(\Sigma, \theta_0^{\text{perfo}}, g^{(1)}) = (\Sigma + \tau I_p)^{-1} \Sigma \left[\theta_0^{\text{perfo}} + \frac{\Sigma^{-1/2} \gamma^{(1)}(\theta_0^{\text{perfo}}) g^{(1)}}{\sqrt{p}} \right], \quad (32)$$

$$\left(\gamma^{(1)}(\theta_0^{\text{perfo}}) \right)^2 = \kappa \left(\sigma^2 + \tilde{\mathcal{R}}_{\text{eq}}^{(1)}(\Sigma, \theta_0^{\text{perfo}}, \theta_0^{\text{perfo}}) \right), \quad (33)$$

τ is the unique solution of (17) and $g^{(1)} \sim \mathcal{N}(0, I_p)$. By plugging (32) into (31) and computing the expectation with respect to $g^{(1)}$, we get

$$\tilde{\mathcal{R}}_{\text{eq}}^{(1)}(\Sigma, \theta_{\text{pop}}^*, \theta_0^{\text{perfo}}) = \left\| (\Sigma + \tau I_p)^{-1} \Sigma \theta_0^{\text{perfo}} - \theta_{\text{pop}}^* \right\|_{\Sigma}^2 + \frac{\left(\gamma^{(1)}(\theta_0^{\text{perfo}}) \right)^2}{p} \text{Tr} \left[\Sigma^2 (\Sigma + \tau I_p)^{-2} \right]. \quad (34)$$

Next, we solve the fixed point equation in $\gamma^{(1)}(\theta_0^{\text{perfo}})$:

$$\begin{aligned} \left(\gamma^{(1)}(\theta_0^{\text{perfo}}) \right)^2 &= \kappa \left(\sigma^2 + \tilde{\mathcal{R}}_{\text{eq}}^{(1)}(\Sigma, \theta_0^{\text{perfo}}, \theta_0^{\text{perfo}}) \right) \\ &= \kappa \left(\sigma^2 + \left\| \left((\Sigma + \tau I_p)^{-1} \Sigma - I_p \right) \theta_0^{\text{perfo}} \right\|_{\Sigma}^2 + \frac{\left(\gamma^{(1)}(\theta_0^{\text{perfo}}) \right)^2}{p} \text{Tr} \left[\Sigma^2 (\Sigma + \tau I_p)^{-2} \right] \right) \\ &= \kappa \left(\sigma^2 + \tau^2 \left\| (\Sigma + \tau I_p)^{-1} \theta_0^{\text{perfo}} \right\|_{\Sigma}^2 + \frac{\left(\gamma^{(1)}(\theta_0^{\text{perfo}}) \right)^2}{p} \text{Tr} \left[\Sigma^2 (\Sigma + \tau I_p)^{-2} \right] \right). \end{aligned}$$

The last equality comes from

$$I_p - (\Sigma + \tau I_p)^{-1} \Sigma = (\Sigma + \tau I_p)^{-1} (\Sigma + \tau I_p) - (\Sigma + \tau I_p)^{-1} \Sigma = \tau (\Sigma + \tau I_p)^{-1}.$$

Rearranging gives that

$$\left(\gamma^{(1)}(\theta_0^{\text{perfo}}) \right)^2 = \kappa \frac{\sigma^2 + \tau^2 \left\| (\Sigma + \tau I_p)^{-1} \theta_0^{\text{perfo}} \right\|_{\Sigma}^2}{1 - \frac{1}{n} \text{Tr} \left[\Sigma^2 (\Sigma + \tau I_p)^{-2} \right]}, \quad (35)$$

which plugged into (34) gives the desired result. \square

We note that the expression in (30) depends on θ_0 and, in fact, it keeps depending on it even after neglecting terms of order $O(\|D\|_{\text{op}}^2)$.

Deterministic equivalent for $\mathcal{R}_2(\Sigma, \theta_2, \theta_{\text{pop}}^*)$. Next, by iterating twice the strategy of Lemma 7, we derive a deterministic equivalent for $\mathcal{R}_2(\Sigma, \theta_2, \theta_{\text{pop}}^*)$.

Lemma 8. *Let $R > 0$ be a constant such that $\theta_{\text{pop}}^*, \theta_0 \in B_p(R)$. Assume that $\kappa, \sigma, \lambda \in (1/M, M)$ and $\|\Sigma\|_{\text{op}}, \|\Sigma^{-1}\|_{\text{op}} \leq M$ for some constant $M > 1$. Then, there exists a constant $C = C(M, R)$ such that, for any $\delta \in (0, 1/2]$, the following holds*

$$\sup_{\theta_{\text{pop}}^*, \theta_0 \in B_p(R)} \Pr \left(\left| \mathcal{R}_2(\Sigma, \theta_2, \theta_{\text{pop}}^*) - \mathcal{R}_{\text{eq}}^{(2)}(\Sigma, \theta_0, \theta_{\text{pop}}^*) \right| \geq \delta \right) \leq C p e^{-p\delta^4/C}, \quad (36)$$

where

$$\begin{aligned} \mathcal{R}_{\text{eq}}^{(2)}(\Sigma, \theta_0, \theta_{\text{pop}}^*) &= \left\| (\Sigma + \tau I_p)^{-1} \Sigma D (\Sigma + \tau I_p)^{-1} \Sigma (\theta_{\text{pop}}^* + D\theta_0) - \tau (\Sigma + \tau I_p)^{-1} \theta_{\text{pop}}^* \right\|_{\Sigma}^2 \\ &+ \kappa \text{Tr} \left[\Sigma (\Sigma + \tau I_p)^{-2} D \Sigma^3 (\Sigma + \tau I_p)^{-2} D \right] \frac{\sigma^2 + \tau^2 \|(\Sigma + \tau I_p)^{-1} (\theta_{\text{pop}}^* + D\theta_0)\|_{\Sigma}^2}{p - \kappa \text{Tr} \left[\Sigma^2 (\Sigma + \tau I_p)^{-2} \right]} \\ &+ \kappa \text{Tr} \left[\Sigma^2 (\Sigma + \tau I_p)^{-2} \right] \frac{\sigma^2 + \tau^2 \|(\Sigma + \tau I_p)^{-1} (\theta_{\text{pop}}^* + D(\Sigma + \tau I_p)^{-1} \Sigma (\theta_{\text{pop}}^* + D\theta_0))\|_{\Sigma}^2}{p - \kappa \text{Tr} \left[\Sigma^2 (\Sigma + \tau I_p)^{-2} \right]} \\ &+ \kappa^2 \tau^2 \text{Tr} \left[\Sigma^2 (\Sigma + \tau I_p)^{-2} \right] \text{Tr} \left[\Sigma (\Sigma + \tau I_p)^{-2} D \Sigma (\Sigma + \tau I_p)^{-2} D \right] \\ &\cdot \frac{\sigma^2 + \tau^2 \|(\Sigma + \tau I_p)^{-1} (\theta_{\text{pop}}^* + D\theta_0)\|_{\Sigma}^2}{(p - \kappa \text{Tr} \left[\Sigma^2 (\Sigma + \tau I_p)^{-2} \right])^2}, \end{aligned} \quad (37)$$

and τ is the unique solution of (17).

Proof. The proof extends the argument of Theorem 2 by (Ildiz et al., 2025) to the ridge regression case, and it applies the distributional characterization of the minimum norm interpolator by Han & Xu (2023) twice. First, note that $\|\theta_1\|_2$ is bounded by a constant $C_1 = C_1(R, M)$ independent of n, p , with probability at least $C_2 e^{-p/C_2}$, where $C_2 = C_2(R, M)$ is a constant independent of n, p . This follows from a direct adaptation of Proposition 11 by Ildiz et al. (2025). Define $R' := \max(C_1, \|\theta_{\text{pop}}^*\|_2)$. Then, upon conditioning on θ_1 , we can apply Lemma 7 (after re-defining R to be R'), which gives that, for some constant $C_3 = C_3(R, M)$,

$$\sup_{\theta_{\text{pop}}^*, \theta_1 \in B_p(R')} \Pr \left(\left| \mathcal{R}_2(\Sigma, \theta_2, \theta_{\text{pop}}^*) - \mathcal{R}_{\text{eq}}^{(1)}(\Sigma, \theta_1, \theta_{\text{pop}}^*) \right| \geq \delta \right) \leq C_3 p e^{-p\delta^4/C_3}, \quad (38)$$

where $\mathcal{R}_{\text{eq}}^{(1)}(\Sigma, \theta_1, \theta_{\text{pop}}^*)$ is defined in (30) and τ is the unique solution of (17).

We now evaluate the first term in the expression for $\mathcal{R}_{\text{eq}}^{(1)}(\Sigma, \theta_1, \theta_{\text{pop}}^*)$:

$$\begin{aligned} \mathcal{R}_{\text{eq},1}^{(1)}(\Sigma, \theta_1, \theta_{\text{pop}}^*) &:= \left\| (\Sigma + \tau I_p)^{-1} \Sigma (\theta_{\text{pop}}^* + D\theta_1) - \theta_{\text{pop}}^* \right\|_{\Sigma}^2 \\ &= \left\| (\Sigma + \tau I_p)^{-1} \Sigma D\theta_1 - \tau (\Sigma + \tau I_p)^{-1} \theta_{\text{pop}}^* \right\|_{\Sigma}^2. \end{aligned}$$

Let $M_1 = \Sigma^{1/2}$, $M_2 = (\Sigma + \tau I_p)^{-1} \Sigma D$ and $a = \tau (\Sigma + \tau I_p)^{-1} \theta_{\text{pop}}^*$. Then, the function $\theta_1 \mapsto \mathcal{R}_{\text{eq},1}^{(1)}(\Sigma, \theta_1, \theta_{\text{pop}}^*)$ can be expressed as

$$f(\theta_1) = \|M_1(M_2\theta_1 - a)\|_2^2,$$

which has gradient

$$\nabla f(\theta_1) = 2M_2^\top M_1^\top M_1(M_2\theta_1 - a).$$

As $\|\theta_1\|_2 \leq C_1$, f is Lipschitz and its Lipschitz constant is $2\|M_1\|_{\text{op}}^2 \|M_2\|_{\text{op}} (\|M_1\|_{\text{op}} C_1 + \|a\|_2)$. As $\|M_1\|_{\text{op}}, \|M_2\|_{\text{op}}, C_1, \|a\|_2$ are all upper bounded by constants dependent only on R, M , the Lipschitz constant of f is also upper bounded by a constant dependent only on R, M . Thus, an

application of the distributional characterization by Han & Xu (2023) (restated as Theorem 4 in (Ildiz et al., 2025)) gives that, for some constant $C_4 = C_4(R, M)$,

$$\sup_{\theta_{\text{pop}}^*, \theta_1 \in B_p(R')} \Pr \left(\left| \mathcal{R}_{\text{eq},1}^{(1)}(\Sigma, \theta_1, \theta_{\text{pop}}^*) - \tilde{\mathcal{R}}_{\text{eq},1}^{(1)}(\Sigma, \theta_{\text{pop}}^*, \theta_0^{\text{perfo}}) \right| \geq \delta \right) \leq C_4 p e^{-p\delta^4/C_4}, \quad (39)$$

where

$$\tilde{\mathcal{R}}_{\text{eq},1}^{(1)}(\Sigma, \theta_{\text{pop}}^*, \theta_0^{\text{perfo}}) = \mathbb{E}_{g^{(1)}} \left[\left\| (\Sigma + \tau I_p)^{-1} \Sigma D X^{(1)} \left(\Sigma, \theta_0^{\text{perfo}}, g^{(1)} \right) - \tau (\Sigma + \tau I_p)^{-1} \theta_{\text{pop}}^* \right\|_{\Sigma}^2 \right]. \quad (40)$$

We recall from Lemma 7 that $\theta_0^{\text{perfo}} = \theta_{\text{pop}}^* + D\theta_0$, $g^{(1)} \sim \mathcal{N}(0, I_p)$ and $X^{(1)}(\Sigma, \theta_0^{\text{perfo}}, g^{(1)})$ is given by (32). By plugging (32) into the RHS of (40) and computing the expectation with respect to $g^{(1)}$, we have

$$\begin{aligned} \tilde{\mathcal{R}}_{\text{eq},1}^{(1)}(\Sigma, \theta_{\text{pop}}^*, \theta_0^{\text{perfo}}) &= \mathbb{E}_{g^{(1)}} \left[\left\| (\Sigma + \tau I_p)^{-1} \Sigma D (\Sigma + \tau I_p)^{-1} \Sigma \theta_0^{\text{perfo}} - \tau (\Sigma + \tau I_p)^{-1} \theta_{\text{pop}}^* \right. \right. \\ &\quad \left. \left. + (\Sigma + \tau I_p)^{-1} \Sigma D (\Sigma + \tau I_p)^{-1} \Sigma^{1/2} \frac{\gamma^{(1)}(\theta_0^{\text{perfo}}) g^{(1)}}{\sqrt{p}} \right\|_{\Sigma}^2 \right] \\ &= \left\| (\Sigma + \tau I_p)^{-1} \Sigma D (\Sigma + \tau I_p)^{-1} \Sigma \theta_0^{\text{perfo}} - \tau (\Sigma + \tau I_p)^{-1} \theta_{\text{pop}}^* \right\|_{\Sigma}^2 \\ &\quad + \frac{\left(\gamma^{(1)}(\theta_0^{\text{perfo}}) \right)^2}{p} \text{Tr} \left[\Sigma (\Sigma + \tau I_p)^{-2} D \Sigma^3 (\Sigma + \tau I_p)^{-2} D \right], \end{aligned} \quad (41)$$

where in the last step we have used the circulant property of the trace. By using the expression for $\gamma^{(1)}(\theta_0^{\text{perfo}})$ in (35) and recalling that $\theta_0^{\text{perfo}} = \theta_{\text{pop}}^* + D\theta_0$, one readily obtains that the RHS of (41) coincides with the first two lines of the RHS of (37).

Finally, we evaluate the second term in the expression for $\mathcal{R}_{\text{eq}}^{(1)}(\Sigma, \theta_1, \theta_{\text{pop}}^*)$:

$$\mathcal{R}_{\text{eq},2}^{(1)}(\Sigma, \theta_1, \theta_{\text{pop}}^*) := \kappa \text{Tr} \left[\Sigma^2 (\Sigma + \tau I_p)^{-2} \right] \frac{\sigma^2 + \tau^2 \left\| (\Sigma + \tau I_p)^{-1} (\theta_{\text{pop}}^* + D\theta_1) \right\|_{\Sigma}^2}{p - \kappa \text{Tr} \left[\Sigma^2 (\Sigma + \tau I_p)^{-2} \right]}.$$

Let $M_1 = \Sigma^{1/2}$, $M_2 = (\Sigma + \tau I_p)^{-1} D$ and $a = (\Sigma + \tau I_p)^{-1} \theta_{\text{pop}}^*$. Then, the function $\theta_1 \mapsto \left\| (\Sigma + \tau I_p)^{-1} (\theta_{\text{pop}}^* + D\theta_1) \right\|_{\Sigma}^2$ can be expressed as

$$f(\theta_1) = \|M_1(M_2\theta_1 + a)\|_2^2,$$

which has gradient

$$\nabla f(\theta_1) = 2M_2^{\top} M_1^{\top} M_1(M_2\theta_1 + a).$$

As $\|\theta_1\|_2 \leq C_1$, f is Lipschitz and its Lipschitz constant is $2\|M_1\|_{\text{op}}^2 \|M_2\|_{\text{op}} (\|M_1\|_{\text{op}} C_1 + \|a\|_2)$. As $\|M_1\|_{\text{op}}$, $\|M_2\|_{\text{op}}$, C_1 , $\|a\|_2$ are all upper bounded by constants dependent only on R, M , the Lipschitz constant of f is also upper bounded by a constant dependent only on R, M . Note that the quantity $|p - \kappa \text{Tr} [\Sigma^2 (\Sigma + \tau I_p)^{-2}]|$ is lower bounded by a constant dependent only on R, M , as a consequence of Proposition 2.1 in Han & Xu (2023). Thus, we have that the function $\theta_1 \mapsto \mathcal{R}_{\text{eq},2}^{(1)}(\Sigma, \theta_1, \theta_{\text{pop}}^*)$ is Lipschitz and its Lipschitz constant is $C_5 = C_5(R, M)$. Hence, another application of the distributional characterization by Han & Xu (2023) (cf. Theorem 4 in (Ildiz et al., 2025)) gives that, for some constant $C_6 = C_6(R, M)$,

$$\sup_{\theta_{\text{pop}}^*, \theta_1 \in B_p(R')} \Pr \left(\left| \mathcal{R}_{\text{eq},2}^{(1)}(\Sigma, \theta_1, \theta_{\text{pop}}^*) - \tilde{\mathcal{R}}_{\text{eq},2}^{(1)}(\Sigma, \theta_{\text{pop}}^*, \theta_0^{\text{perfo}}) \right| \geq \delta \right) \leq C_6 p e^{-p\delta^4/C_6}, \quad (42)$$

where

$$\begin{aligned} \tilde{\mathcal{R}}_{\text{eq},2}^{(1)}\left(\Sigma, \theta_{\text{pop}}^*, \theta_0^{\text{perfo}}\right) &= \kappa \operatorname{Tr}\left[\Sigma^2(\Sigma + \tau I_p)^{-2}\right] \\ &\cdot \frac{\sigma^2 + \tau^2 \mathbb{E}_{g^{(1)}}\left[\left\|(\Sigma + \tau I_p)^{-1}\left(\theta_{\text{pop}}^* + DX^{(1)}\left(\Sigma, \theta_0^{\text{perfo}}, g^{(1)}\right)\right)\right\|_{\Sigma}^2\right]}{p - \kappa \operatorname{Tr}\left[\Sigma^2(\Sigma + \tau I_p)^{-2}\right]}. \end{aligned} \quad (43)$$

By using (32) and computing the expectation with respect to $g^{(1)}$, we have

$$\begin{aligned} &\mathbb{E}_{g^{(1)}}\left[\left\|(\Sigma + \tau I_p)^{-1}\left(\theta_{\text{pop}}^* + DX^{(1)}\left(\Sigma, \theta_0^{\text{perfo}}, g^{(1)}\right)\right)\right\|_{\Sigma}^2\right] \\ &= \mathbb{E}_{g^{(1)}}\left[\left\|(\Sigma + \tau I_p)^{-1}\theta_{\text{pop}}^* + (\Sigma + \tau I_p)^{-1}D(\Sigma + \tau I_p)^{-1}\Sigma\theta_0^{\text{perfo}}\right.\right. \\ &\quad \left.\left. + (\Sigma + \tau I_p)^{-1}D(\Sigma + \tau I_p)^{-1}\Sigma^{1/2}\frac{\gamma^{(1)}(\theta_0^{\text{perfo}})g^{(1)}}{\sqrt{p}}\right\|_{\Sigma}^2\right] \quad (44) \\ &= \left\|(\Sigma + \tau I_p)^{-1}\theta_{\text{pop}}^* + (\Sigma + \tau I_p)^{-1}D(\Sigma + \tau I_p)^{-1}\Sigma\theta_0^{\text{perfo}}\right\|_{\Sigma}^2 \\ &\quad + \frac{\left(\gamma^{(1)}(\theta_0^{\text{perfo}})\right)^2}{p} \operatorname{Tr}\left[\Sigma(\Sigma + \tau I_p)^{-2}D\Sigma(\Sigma + \tau I_p)^{-2}D\right], \end{aligned}$$

where in the last step we have used the circulant property of the trace. By plugging (44) into (43), using the expression for $\gamma^{(1)}(\theta_0^{\text{perfo}})$ in (35) and recalling that $\theta_0^{\text{perfo}} = \theta_{\text{pop}}^* + D\theta_0$, one readily obtains that the RHS of (43) coincides with the last two lines of the RHS of (37). As $\mathcal{R}_{\text{eq}}^{(1)}\left(\Sigma, \theta_1, \theta_{\text{pop}}^*\right) = \mathcal{R}_{\text{eq},1}^{(1)}\left(\Sigma, \theta_1, \theta_{\text{pop}}^*\right) + \mathcal{R}_{\text{eq},2}^{(1)}\left(\Sigma, \theta_1, \theta_{\text{pop}}^*\right)$, the desired result readily follows by combining (38), (39) and (42). \square

Concluding the argument. Note that

$$\begin{aligned} \operatorname{Tr}\left[\Sigma(\Sigma + \tau I_p)^{-2}D\Sigma^3(\Sigma + \tau I_p)^{-2}D\right] &= O(\|D\|_{\text{op}}^2), \\ \operatorname{Tr}\left[\Sigma(\Sigma + \tau I_p)^{-2}D\Sigma(\Sigma + \tau I_p)^{-2}D\right] &= O(\|D\|_{\text{op}}^2). \end{aligned}$$

Furthermore, we have

$$\begin{aligned} &\left\|(\Sigma + \tau I_p)^{-1}\Sigma D(\Sigma + \tau I_p)^{-1}\Sigma(\theta_{\text{pop}}^* + D\theta_0) - \tau(\Sigma + \tau I_p)^{-1}\theta_{\text{pop}}^*\right\|_{\Sigma}^2 \\ &= \left\|(\Sigma + \tau I_p)^{-1}\Sigma D(\Sigma + \tau I_p)^{-1}\Sigma\theta_{\text{pop}}^* - \tau(\Sigma + \tau I_p)^{-1}\theta_{\text{pop}}^*\right\|_{\Sigma}^2 + O(\|D\|_{\text{op}}^2) \\ &= \left\|\tau(\Sigma + \tau I_p)^{-1}\theta_{\text{pop}}^*\right\|_{\Sigma}^2 \\ &\quad - 2\tau\langle(\Sigma + \tau I_p)^{-1}\theta_{\text{pop}}^*, \Sigma(\Sigma + \tau I_p)^{-1}\Sigma D(\Sigma + \tau I_p)^{-1}\Sigma\theta_{\text{pop}}^*\rangle + O(\|D\|_{\text{op}}^2) \\ &= \tau\langle\theta_{\text{pop}}^*, (\Sigma + \tau I_p)^{-1}(\tau I_p - 2(\Sigma + \tau I_p)^{-1}\Sigma^2 D)\Sigma(\Sigma + \tau I_p)^{-1}\theta_{\text{pop}}^*\rangle + O(\|D\|_{\text{op}}^2). \end{aligned}$$

Similarly, we have

$$\begin{aligned} &\left\|(\Sigma + \tau I_p)^{-1}\left(\theta_{\text{pop}}^* + D(\Sigma + \tau I_p)^{-1}\Sigma(\theta_{\text{pop}}^* + D\theta_0)\right)\right\|_{\Sigma}^2 \\ &= \left\|(\Sigma + \tau I_p)^{-1}\left(\theta_{\text{pop}}^* + D(\Sigma + \tau I_p)^{-1}\Sigma\theta_{\text{pop}}^*\right)\right\|_{\Sigma}^2 + O(\|D\|_{\text{op}}^2) \\ &= \left\|(\Sigma + \tau I_p)^{-1}\theta_{\text{pop}}^*\right\|_{\Sigma}^2 + 2\langle(\Sigma + \tau I_p)^{-1}\theta_{\text{pop}}^*, \Sigma(\Sigma + \tau I_p)^{-1}D(\Sigma + \tau I_p)^{-1}\Sigma\theta_{\text{pop}}^*\rangle + O(\|D\|_{\text{op}}^2) \\ &= \langle\theta_{\text{pop}}^*, (\Sigma + \tau I_p)^{-1}(I_p + 2(\Sigma + \tau I_p)^{-1}\Sigma D)\Sigma(\Sigma + \tau I_p)^{-1}\theta_{\text{pop}}^*\rangle + O(\|D\|_{\text{op}}^2). \end{aligned}$$

Recalling the definitions (16) and (37), we conclude that

$$\mathcal{R}_{\text{eq}}^{(2)}\left(\Sigma, \theta_0, \theta_{\text{pop}}^*\right) = \mathcal{R}_{\text{eq}}\left(\Sigma, \theta_{\text{pop}}^*, D, \lambda\right) + O(\|D\|_{\text{op}}^2). \quad (45)$$

Thus, the desired result follows from (45) and Lemma 8.

C PROOF OF THEOREM 4

We start by computing explicitly $\mathbb{E}_{\theta_{\text{pop}}^*} \mathcal{R}_{\text{eq}}(\Sigma, \theta_{\text{pop}}^*, D, \lambda)$.

Lemma 9. *Consider the setting of Theorem 3, assume that a has covariance I_d/d , and let $\Sigma = \begin{bmatrix} I_d & \rho I_d \\ \rho I_d & I_d \end{bmatrix}$. Then, we have that*

$$\begin{aligned} \mathbb{E}_{\theta_{\text{pop}}^*} \mathcal{R}_{\text{eq}}(\Sigma, \theta_{\text{pop}}^*, D, \lambda) &= \tilde{\mathcal{R}}(D, \lambda, \rho) + O(\bar{b}\rho^2 + \rho^4), \\ \tilde{\mathcal{R}}(D, \lambda, \rho) &:= \mathcal{R}_0(\lambda, \rho) + \bar{b}A_1(\lambda) + \bar{c}\rho^2 A_2(\lambda), \end{aligned}$$

where $\bar{b} = \text{Tr}[\text{diag}(b)]/d$, $\bar{c} = \text{Tr}[\text{diag}(c)]/d$ and the auxiliary functions $\mathcal{R}_0(\lambda, \rho)$, $A_1(\lambda)$, and $A_2(\lambda)$ are given by

$$\begin{aligned} \mathcal{R}_0(\lambda, \rho) &= \frac{\tau^2}{(1+\tau)^2} + \frac{\kappa}{(1+\tau)^2 - \kappa} \left(\sigma^2 + \frac{\tau^2}{(1+\tau)^2} \right) \\ &\quad + \rho^2 \left(\frac{\tau^2(1-2\tau)}{(1+\tau)^4} + \frac{\kappa\tau^2(1-2\tau)}{(1+\tau)^4((1+\tau)^2 - \kappa)} + \frac{\kappa\tau(\tau-2)}{((1+\tau)^2 - \kappa)^2} \left(\sigma^2 + \frac{\tau^2}{(1+\tau)^2} \right) \right), \\ A_1(\lambda) &= -\frac{2\tau}{(1+\tau)^3} + \frac{2\kappa\tau^2}{(1+\tau)^3((1+\tau)^2 - \kappa)}, \\ A_2(\lambda) &= -\frac{4\tau^3}{(1+\tau)^5} + \frac{2\kappa\tau^3(\tau^2 - 1)}{(1+\tau)^6((1+\tau)^2 - \kappa)}. \end{aligned} \tag{46}$$

Proof. Given a $p \times p$ matrix M , let us denote by $(M)_1$ its top-left $d \times d$ block. For any $M \in \mathbb{R}^{p \times p}$, we have

$$\begin{aligned} \mathbb{E}_{\theta_{\text{pop}}^*} [\langle \theta_{\text{pop}}^*, M\theta_{\text{pop}}^* \rangle] &= \mathbb{E}_{\theta_{\text{pop}}^*} [(\theta_{\text{pop}}^*)^\top M\theta_{\text{pop}}^*] = \mathbb{E}_{\theta_{\text{pop}}^*} [\text{Tr}[(\theta_{\text{pop}}^*)^\top M\theta_{\text{pop}}^*]] \\ &= \mathbb{E}_{\theta_{\text{pop}}^*} [\text{Tr}[M\theta_{\text{pop}}^*(\theta_{\text{pop}}^*)^\top]] = \text{Tr}[(M)_1]/d, \end{aligned}$$

where the third equality uses the circulant property of the trace and the last one that $(\theta_{\text{pop}}^*)^\top = (a^\top, 0)$ with a having covariance I_d/d . Thus, from (16), we have

$$\begin{aligned} \mathbb{E}_{\theta_{\text{pop}}^*} \mathcal{R}_{\text{eq}}(\Sigma, \theta_{\text{pop}}^*, D, \lambda) &= \frac{\tau^2}{d} \text{Tr} \left[\left(\Sigma (\Sigma + \tau I_p)^{-2} \right)_1 \right] \\ &\quad + \kappa \text{Tr} \left[\Sigma^2 (\Sigma + \tau I_p)^{-2} \right] \frac{\sigma^2 + \frac{\tau^2}{d} \text{Tr} \left[\left(\Sigma (\Sigma + \tau I_p)^{-2} \right)_1 \right]}{p - \kappa \text{Tr} \left[\Sigma^2 (\Sigma + \tau I_p)^{-2} \right]} \\ &\quad - \frac{2\tau}{d} \text{Tr} \left[\left((\Sigma + \tau I_p)^{-2} \Sigma^2 D (\Sigma + \tau I_p)^{-1} \Sigma \right)_1 \right] \\ &\quad + \frac{2\kappa\tau^2}{d} \text{Tr} \left[\Sigma^2 (\Sigma + \tau I_p)^{-2} \right] \frac{\text{Tr} \left[\left((\Sigma + \tau I_p)^{-2} \Sigma D (\Sigma + \tau I_p)^{-1} \Sigma \right)_1 \right]}{p - \kappa \text{Tr} \left[\Sigma^2 (\Sigma + \tau I_p)^{-2} \right]}. \end{aligned} \tag{47}$$

Note that $\Sigma + \tau I_p = \begin{bmatrix} 1+\tau & \rho \\ \rho & 1+\tau \end{bmatrix} \otimes I_d$ has inverse $(\Sigma + \tau I_p)^{-1} = \frac{1}{(1+\tau)^2 - \rho^2} \begin{bmatrix} 1+\tau & -\rho \\ -\rho & 1+\tau \end{bmatrix} \otimes I_d$. Furthermore,

$$\begin{aligned} (\Sigma + \tau I_p)^{-2} &= \frac{1}{((1+\tau)^2 - \rho^2)^2} \begin{bmatrix} (1+\tau)^2 + \rho^2 & -2\rho(1+\tau) \\ -2\rho(1+\tau) & (1+\tau)^2 + \rho^2 \end{bmatrix} \otimes I_d, \\ \Sigma^2 &= \begin{bmatrix} 1+\rho^2 & 2\rho \\ 2\rho & 1+\rho^2 \end{bmatrix} \otimes I_d. \end{aligned}$$

A direct block multiplication gives

$$\begin{aligned}
\text{Tr} \left[(\Sigma(\Sigma + \tau I_p)^{-2})_1 \right] &= d \frac{(1 + \tau)^2 - \rho^2(1 + 2\tau)}{((1 + \tau)^2 - \rho^2)^2}, \\
\text{Tr} \left[\Sigma^2(\Sigma + \tau I_p)^{-2} \right] &= 2d \frac{(1 + \tau - \rho^2)^2 + \rho^2\tau^2}{((1 + \tau)^2 - \rho^2)^2}, \\
\text{Tr} \left[((\Sigma + \tau I_p)^{-2}\Sigma^2 D(\Sigma + \tau I_p)^{-1}\Sigma)_1 \right] &= \frac{(1 + \tau - \rho^2) ((1 + \tau - \rho^2)^2 + \rho^2\tau^2)}{((1 + \tau)^2 - \rho^2)^3} \text{Tr}[\text{diag}(b)] \\
&\quad + \frac{2(1 + \tau - \rho^2)\rho^2\tau^2}{((1 + \tau)^2 - \rho^2)^3} \text{Tr}[\text{diag}(c)], \\
\text{Tr} \left[((\Sigma + \tau I_p)^{-2}\Sigma D(\Sigma + \tau I_p)^{-1}\Sigma)_1 \right] &= \frac{(1 + \tau - \rho^2) ((1 + \tau)(1 + \tau - \rho^2) - \rho^2\tau)}{((1 + \tau)^2 - \rho^2)^3} \text{Tr}[\text{diag}(b)] \\
&\quad + \frac{\rho^2\tau (\rho^2 + \tau^2 - 1)}{((1 + \tau)^2 - \rho^2)^3} \text{Tr}[\text{diag}(c)].
\end{aligned}$$

Expanding each rational function at $\rho = 0$ using

$$\begin{aligned}
\frac{1}{((1 + \tau)^2 - \rho^2)^2} &= \frac{1}{(1 + \tau)^4} \left(1 + \frac{2\rho^2}{(1 + \tau)^2} \right) + O(\rho^4), \\
\frac{1}{((1 + \tau)^2 - \rho^2)^3} &= \frac{1}{(1 + \tau)^6} \left(1 + \frac{3\rho^2}{(1 + \tau)^2} \right) + O(\rho^4),
\end{aligned}$$

yields, to order ρ^2 ,

$$\begin{aligned}
\frac{1}{d} \text{Tr} \left[(\Sigma(\Sigma + \tau I_p)^{-2})_1 \right] &= \left(\frac{1}{(1 + \tau)^2} + \rho^2 \frac{1 - 2\tau}{(1 + \tau)^4} \right) + O(\rho^4), \\
\frac{1}{d} \text{Tr} \left[\Sigma^2(\Sigma + \tau I_p)^{-2} \right] &= \frac{2}{(1 + \tau)^2} + 2\rho^2 \frac{\tau^2 - 2\tau}{(1 + \tau)^4} + O(\rho^4), \\
\frac{1}{d} \text{Tr} \left[((\Sigma + \tau I_p)^{-2}\Sigma^2 D(\Sigma + \tau I_p)^{-1}\Sigma)_1 \right] &= \frac{\bar{b}}{(1 + \tau)^3} + \rho^2 \left(\frac{\tau^2 - 3\tau}{(1 + \tau)^5} \bar{b} + \frac{2\tau^2}{(1 + \tau)^5} \bar{c} \right) + O(\rho^4), \\
\frac{1}{d} \text{Tr} \left[((\Sigma + \tau I_p)^{-2}\Sigma D(\Sigma + \tau I_p)^{-1}\Sigma)_1 \right] &= \frac{\bar{b}}{(1 + \tau)^3} + \rho^2 \left(\frac{1 - 3\tau}{(1 + \tau)^5} \bar{b} + \frac{\tau(\tau^2 - 1)}{(1 + \tau)^6} \bar{c} \right) + O(\rho^4).
\end{aligned}$$

Moreover, we have that

$$\frac{\kappa \text{tr} [\Sigma^2(\Sigma + \tau I_p)^{-2}]}{p - \kappa \text{tr} [\Sigma^2(\Sigma + \tau I_p)^{-2}]} = \frac{\kappa}{(1 + \tau)^2 - \kappa} + \rho^2 \frac{\kappa\tau(\tau - 2)}{((1 + \tau)^2 - \kappa)^2} + O(\rho^4).$$

Plugging these into (47) gives the claimed result. \square

Let us further define

$$\tau^*(D, \rho) := \arg \min_{\tau \geq 0} \tilde{\mathcal{R}}(D, \lambda, \rho), \quad \tau_0^*(\rho) := \arg \min_{\tau \geq 0} \mathcal{R}_0(\lambda, \rho), \quad \tau_0 := \tau_0^*(0). \quad (48)$$

Then, the following result proves an expression for $\tau^*(D, \rho)$, up to order ρ^2 .

Lemma 10. *In the setting of Theorem 4, we have that*

$$\tau^*(D, \rho) = \tau_0^*(\rho) + \bar{b} (B_3(\sigma, \kappa) + O(\rho^2)) + \bar{c} (\rho^2 C_3(\sigma, \kappa) + O(\rho^4)) + O(\bar{b}^2 + \bar{c}^2),$$

where

$$\begin{aligned}
\tau_0 &= \frac{1 + \kappa + \kappa\sigma^2 + \sqrt{(1 + \kappa + \kappa\sigma^2)^2 - 4\kappa}}{2} - 1, \\
\tau_0^*(\rho) &= \tau_0 - \rho^2 \frac{\kappa\tau_0^2}{(1 + \tau_0)((1 + \tau_0)^2 - \kappa)} + O(\rho^4), \\
B_3(\sigma, \kappa) &= -\frac{2(1 + \tau_0)^4 - 3(\kappa + 1)(1 + \tau_0)^3 + 4\kappa(1 + \tau_0)^2 + \kappa(\kappa + 1)(1 + \tau_0) - 2\kappa^2}{(1 + \tau_0)^2((1 + \tau_0)^2 - \kappa)}, \\
C_3(\sigma, \kappa) &= -\frac{\tau_0^2 (4\tau_0^4 + (6 - 3\kappa)\tau_0^3 - (6 + 3\kappa)\tau_0^2 + (\kappa^2 + 9\kappa - 14)\tau_0 - 3\kappa^2 + 9\kappa - 6)}{(1 + \tau_0)^4((1 + \tau_0)^2 - \kappa)}.
\end{aligned} \quad (49)$$

Proof. A direct differentiation gives

$$\begin{aligned}
\frac{d}{d\tau} \tilde{\mathcal{R}}(D, \lambda, \rho) = & \frac{2}{1+\tau} \left(\frac{\tau}{(1+\tau)^2 - \kappa} - \frac{\kappa (\sigma^2(1+\tau)^2 + \tau^2)}{((1+\tau)^2 - \kappa)^2} \right) \\
& + \rho^2 \left(\frac{2\tau(\tau^2 - 4\tau + 1)}{(1+\tau)^5} + \frac{2\kappa\tau((1+\tau)^2(3\tau^2 - 5\tau + 1) - \kappa(\tau^2 - 4\tau + 1))}{(1+\tau)^5((1+\tau)^2 - \kappa)^2} \right. \\
& \quad \left. - \frac{2\kappa^2(\kappa\sigma^2(\tau - 1)(1+\tau)^3 + \kappa\tau^2(\tau^2 + \tau - 3))}{(1+\tau)^3((1+\tau)^2 - \kappa)^3} \right. \\
& \quad \left. - \frac{2\kappa(\sigma^2(1+\tau)^4(\tau^2 - 4\tau + 1) + \tau^2(1+\tau)^2(\tau^2 - 5\tau + 3))}{(1+\tau)^3((1+\tau)^2 - \kappa)^3} \right) \\
& + \bar{b} \left(\frac{4\tau - 2}{(1+\tau)^4} + \frac{\kappa\tau(4 - 6\tau)}{(1+\tau)^4((1+\tau)^2 - \kappa)} - \frac{4\kappa^2\tau^2}{(1+\tau)^4((1+\tau)^2 - \kappa)^2} \right) \\
& + \bar{c}\rho^2 \left(\frac{4\tau^2(2\tau - 3)}{(1+\tau)^6} + \frac{2\kappa\tau^2(1+\tau)(\kappa(\tau^2 - 6\tau + 3) - (1+\tau)^2(3\tau^2 - 8\tau + 3))}{(1+\tau)^7((1+\tau)^2 - \kappa)^2} \right).
\end{aligned}$$

With this explicit derivatives, the stationarity equation $\frac{d}{d\tau} \tilde{\mathcal{R}}(D, \lambda, \rho) = 0$ is equivalent to $\frac{F(\tau, \bar{b}, \bar{c}, \rho^2)}{(1+\tau)^7((1+\tau)^2 - \kappa)^3} = 0$, where

$$F(\tau, \bar{b}, \bar{c}, \rho^2) = F_0(\tau)\rho^2 F_\rho(\tau) + \bar{b}F_b(\tau) + \bar{c}\rho^2 F_{\rho c}(\tau),$$

$$F_0(\tau) = 2(1+\tau)^7(\kappa - (1+\tau)^2)(\kappa\sigma^2\tau + \kappa\sigma^2 + \kappa\tau - \tau^2 - \tau),$$

$$F_b(\tau) = -2(1+\tau)^4(\kappa - (1+\tau)^2)(\kappa^2\tau - \kappa^2 - 3\kappa\tau^3 - 5\kappa\tau^2 + 2\kappa + 2\tau^4 + 5\tau^3 + 3\tau^2 - \tau - 1),$$

$$\begin{aligned}
F_\rho(\tau) = & -2(1+\tau)^5(\kappa^2\sigma^2\tau^3 + \kappa^2\sigma^2\tau^2 - \kappa^2\sigma^2\tau - \kappa^2\sigma^2 + \kappa^2\tau^3 + \kappa^2\tau^2 - \kappa^2\tau \\
& + \kappa\sigma^2\tau^5 - \kappa\sigma^2\tau^4 - 8\kappa\sigma^2\tau^3 - 8\kappa\sigma^2\tau^2 - \kappa\sigma^2\tau + \kappa\sigma^2 \\
& + \kappa\tau^5 - 4\kappa\tau^4 - 9\kappa\tau^3 - 2\kappa\tau^2 + 2\kappa\tau - \tau^6 + \tau^5 + 8\tau^4 + 8\tau^3 + \tau^2 - \tau).
\end{aligned}$$

$$F_{\rho c}(\tau) = -2\tau^2(1+\tau)^2(\kappa - (1+\tau)^2)(\kappa^2\tau - 3\kappa^2 - 3\kappa\tau^3 - 3\kappa\tau^2 + 9\kappa\tau + 9\kappa + 4\tau^4 + 6\tau^3 - 6\tau^2 - 14\tau - 6).$$

Setting $\bar{b} = \bar{c} = \rho^2 = 0$ yields

$$(1+\tau)^2 - (1 + \kappa + \kappa\sigma^2)(1+\tau) + \kappa = 0,$$

and the desired minimum corresponds to its largest solution, which is given by τ_0 as expressed in the statement. It is easy to see that

$$\begin{aligned}
\partial_\tau F(\tau_0, 0, 0, 0) = & -2(1+\tau_0)^7((1+\tau_0)^2 - \kappa)(2(1+\tau_0) - (1 + \kappa + \kappa\sigma^2)) \\
= & -2(1+\tau_0)^7((1+\tau_0)^2 - \kappa)\sqrt{(1 + \kappa + \kappa\sigma^2)^2 - 4\kappa} \neq 0.
\end{aligned}$$

Therefore, the implicit function theorem gives a smooth map $\tau^*(\bar{b}, \bar{c}, \rho^2)$ with $\tau^*(0, 0, 0) = \tau_0$ and $F(\tau^*, \cdot) = 0$. Differentiating $F = 0$ at $(\tau_0, 0, 0, 0)$ in each small parameter and dividing by $\partial_\tau F(\tau_0, 0, 0, 0)$ yields the linear expansion for $\tau^* - \tau_0$ with the coefficients given earlier. A second differentiation shows the stated $O(\cdot)$ remainder bounds, which completes the proof. \square

As λ and τ are linked by the fixed point equation (17), an application of Lemma 10 readily gives that

$$\lambda_{\text{eq}}^*(D, \rho) = \lambda_{\text{eq}, D=0}^*(\rho) + \bar{b}(B_1(\sigma, \kappa) + O(\rho^2)) + \bar{c}\rho^2(C_1(\sigma, \kappa) + O(\rho^2)) + O(\bar{b}^2 + \bar{c}^2), \quad (50)$$

where

$$\begin{aligned}
\lambda_{\text{eq}, D=0}^*(\rho) &= \tau_0 \left(\kappa^{-1} - \frac{1}{1+\tau_0} \right) + \rho^2 \left(\tau_0 \left(\frac{1}{(1+\tau_0)^2} - \frac{1}{(1+\tau_0)^3} \right) \right. \\
&\quad \left. - \left(\kappa^{-1} - \frac{1}{(1+\tau_0)^2} \right) \frac{\kappa \tau_0^2}{(1+\tau_0)((1+\tau_0)^2 - \kappa)} \right) + O(\rho^4), \\
B_1(\sigma, \kappa) &= -\frac{2(1+\tau_0)^4 - 3(\kappa+1)(1+\tau_0)^3 + 4\kappa(1+\tau_0)^2 + \kappa(\kappa+1)(1+\tau_0) - 2\kappa^2}{\kappa(1+\tau_0)^4}, \\
C_1(\sigma, \kappa) &= -\frac{\tau_0^2 (4\tau_0^4 + (6-3\kappa)\tau_0^3 - (6+3\kappa)\tau_0^2 + (\kappa^2 + 9\kappa - 14)\tau_0 - 3\kappa^2 + 9\kappa - 6)}{\kappa(1+\tau_0)^6}.
\end{aligned} \tag{51}$$

This proves (22). Next, the corollary below proves (23).

Corollary 11. *Consider the setting of Theorem 4 and let τ_0 be given by (49). Then, we have that*

$$\mathcal{R}_{\text{eq}}^*(D, \rho) = \mathcal{R}_{\text{eq}}^*(\rho) + \bar{b}(B_2(\sigma, \kappa) + O(\rho^2)) + \bar{c}\rho^2(C_2(\sigma, \kappa) + O(\rho^2)) + O(\bar{b}^2 + \bar{c}^2), \tag{52}$$

where

$$\begin{aligned}
\mathcal{R}_{\text{eq}}^*(\rho) &= \frac{\tau_0^2}{(1+\tau_0)^2} + \frac{\kappa}{(1+\tau_0)^2 - \kappa} \left(\sigma^2 + \frac{\tau_0^2}{(1+\tau_0)^2} \right) \\
&\quad + \rho^2 \left(\frac{\tau_0^2(1-2\tau_0)}{(1+\tau_0)^4} + \frac{\kappa\tau_0^2(1-2\tau_0)}{(1+\tau_0)^4((1+\tau_0)^2 - \kappa)} \right. \\
&\quad \left. + \frac{\kappa\tau_0(\tau_0-2)}{((1+\tau_0)^2 - \kappa)^2} \left(\sigma^2 + \frac{\tau_0^2}{(1+\tau_0)^2} \right) \right) + O(\rho^4), \\
B_2(\sigma, \kappa) &= -\frac{2\tau_0}{(1+\tau_0)^3} + \frac{2\kappa\tau_0^2}{(1+\tau_0)^3((1+\tau_0)^2 - \kappa)}, \\
C_2(\sigma, \kappa) &= -\frac{4\tau_0^3}{(1+\tau_0)^5} + \frac{2\kappa\tau_0^3(\tau_0^2 - 1)}{(1+\tau_0)^6((1+\tau_0)^2 - \kappa)}.
\end{aligned} \tag{53}$$

Proof. Let us re-define $\tilde{\mathcal{R}}(D, \lambda, \rho)$ given in (46) as $\tilde{\mathcal{R}}(\tau, \bar{b}, \bar{c}, \rho^2)$ to emphasize its dependence on τ, \bar{b}, \bar{c} . By definition of τ_0 , we have $\partial_\tau \tilde{\mathcal{R}}(\tau_0, 0, 0, 0) = 0$. Furthermore, from Lemma 10, we have

$$\tau^*(D, \rho) = \tau_0 + O(\bar{b} + (1+\bar{c})\rho^2).$$

A first-order Taylor expansion of $\tilde{\mathcal{R}}(\tau^*(D, \rho), \bar{b}, \bar{c}, \rho^2)$ around $(\tau; \bar{b}, \bar{c}, \rho^2) = (\tau_0; 0, 0, 0)$ gives

$$\begin{aligned}
\tilde{\mathcal{R}}(\tau^*(D, \rho), \bar{b}, \bar{c}, \rho^2) &= \tilde{\mathcal{R}}(\tau_0, \bar{b}, \bar{c}, \rho^2) + \partial_\tau \tilde{\mathcal{R}}(\tau_0, 0, 0, 0)(\tau^*(D, \rho) - \tau_0) \\
&\quad + O((\tau^*(D, \rho) - \tau_0)\bar{b}) + O((\tau^*(D, \rho) - \tau_0)\rho^2) + O(\bar{b}^2 + \bar{c}^2 + \rho^4).
\end{aligned}$$

As $\partial_\tau \tilde{\mathcal{R}}(\tau_0, 0, 0, 0) = 0$, we conclude that

$$\tilde{\mathcal{R}}(\tau^*, \bar{b}, \bar{c}, \rho^2) = \tilde{\mathcal{R}}(\tau_0, \bar{b}, \bar{c}, \rho^2) + O(\bar{b}^2 + \bar{c}^2 + \rho^4),$$

and substituting $\tau = \tau_0$ in (46) gives the claimed expansion. \square

We now move to the proof of (24), which follows from the lemma below.

Lemma 12. *Let $B_1(\sigma, \kappa)$ be given by (51). Then, for any $\kappa > 1$, $B_1(\kappa, \cdot)$ has exactly one zero $\sigma_{B_1}(\kappa) > 0$, with*

$$B_1(\kappa, \sigma) \geq 0 \text{ for } 0 \leq \sigma \leq \sigma_{B_1}(\kappa), \quad B_1(\kappa, \sigma) \leq 0 \text{ for } \sigma \geq \sigma_{B_1}(\kappa).$$

Moreover, as $\kappa \rightarrow \infty$,

$$\sigma_{B_1}^2(\kappa) = \frac{1}{2} - \frac{7}{18}\kappa^{-1} + O(\kappa^{-2}).$$

Proof. Let us define the shorthands

$$s(\sigma) := 1 + \tau_0, \quad N_{B_1}(s, \kappa) := 2s^4 - 3(\kappa + 1)s^3 + 4\kappa s^2 + \kappa(\kappa + 1)s - 2\kappa^2, \quad (54)$$

with τ_0 given by (49). Note that

$$s(\sigma) = \frac{1 + \kappa + \kappa\sigma^2 + \sqrt{(1 + \kappa + \kappa\sigma^2)^2 - 4\kappa}}{2} \geq \frac{1 + \kappa + \sqrt{(1 + \kappa)^2 - 4\kappa}}{2} = \kappa.$$

Now let us also define $\Phi(s) := -N_{B_1}(s, \kappa) / (\kappa s^4)$ for $s \geq \kappa$. A direct calculation gives the factorization

$$\frac{d}{ds} \Phi(s) = \frac{-N'_{B_1}(s)s + 4N_{B_1}(s)}{\kappa s^5} = \frac{-(s^2 - \kappa)(3(\kappa + 1)s - 8\kappa)}{\kappa s^5}.$$

For $s \geq \kappa$ we have $s^2 - \kappa > 0$, hence $\Phi'(s)$ changes sign only once at $s_* := \frac{8\kappa}{3(\kappa+1)}$. If $\kappa \geq 5/3$, then $s_* \leq \kappa$ and Φ is strictly decreasing on $[\kappa, \infty)$. If $1 < \kappa < 5/3$, then $\kappa < s_*$ and Φ is increasing on $[\kappa, s_*)$ and strictly decreasing on (s_*, ∞) .

Note that $B_1(\kappa, \sigma) = -N_{B_1}(s(\sigma), \kappa) / (\kappa s(\sigma)^4) = \Phi(s(\sigma))$ $s(\sigma)$ is strictly increasing in σ , and $\Phi(s(\sigma)) \rightarrow -2/\kappa$ as $\sigma \rightarrow \infty$ (since $s(\sigma) \rightarrow \kappa\sigma^2$ and $N_{B_1}(s, \kappa) \rightarrow 2s^4$). Furthermore, $s(0) = \kappa$ and

$$N_{B_1}(\kappa, \kappa) = -\kappa^2(\kappa - 1)^2 < 0 \implies B_1(\kappa, 0) = -\frac{N_{B_1}(\kappa, \kappa)}{\kappa^5} > 0.$$

Therefore, $B_1(\kappa, \sigma)$ is strictly decreasing on $[0, \infty)$ if $\kappa \geq 5/3$, and for $1 < \kappa < 5/3$ it increases for small σ and then strictly decreases; in either case, since $B_1(\kappa, 0) > 0$ and $\lim_{\sigma \rightarrow \infty} B_1(\kappa, \sigma) = -2/\kappa < 0$, it crosses 0 exactly once, which proves the existence and uniqueness of $\sigma_{B_1}(\kappa)$. At the crossing $B_1(\kappa, \sigma_{B_1}) = 0$, hence $N_{B_1}(s(\sigma_{B_1}), \kappa) = 0$.

Now let $\varepsilon := \kappa^{-1}$ and write $s = \kappa c$. Dividing $N_{B_1}(\kappa c, \kappa) = 0$ by κ^4 yields the analytic equation

$$F(\varepsilon, c) = 0, \quad F(\varepsilon, c) := 2c^4 - 3(1 + \varepsilon)c^3 + 4\varepsilon c^2 + (\varepsilon + \varepsilon^2)c - 2\varepsilon^2.$$

At $\varepsilon = 0$, $F(0, c) = 2c^4 - 3c^3$ has the positive root $c_0 = \frac{3}{2}$, and $\partial_c F(0, c_0) = 8c_0^3 - 9c_0^2 = \frac{27}{4} \neq 0$. By the implicit function theorem there exists a unique analytic branch $c(\varepsilon)$ with $c(0) = \frac{3}{2}$, having the expansion $c(\varepsilon) = \frac{3}{2} + c_1\varepsilon + O(\varepsilon^2)$. Substituting into $F(\varepsilon, c) = 0$ gives that, up to first order,

$$\frac{27}{4}c_1 + \frac{3}{8} = 0 \implies c_1 = -\frac{1}{18}.$$

Thus,

$$\sigma_{B_1}^2 = \frac{(s_c - 1)(s_c - \kappa)}{\kappa s_c} = \left(1 - \frac{1}{\kappa c(\varepsilon)}\right)(c(\varepsilon) - 1),$$

with $s_c = \kappa c(\varepsilon) = \frac{3}{2}\kappa - \frac{1}{18} + O(\kappa^{-1})$. Substituting $c(\varepsilon) = \frac{3}{2} - \frac{1}{18}\varepsilon + O(\varepsilon^2)$ and expanding yields

$$\sigma_{B_1}^2 = \frac{1}{2} - \frac{7}{18}\kappa^{-1} + O(\kappa^{-2}).$$

The analyticity of $c(\varepsilon)$ implies the remainder $O(\varepsilon^2)$ in c and, consequently, the remainder $O(\kappa^{-2})$ in the displayed expansion. \square

Next, we move to the proof of (25), which follows from the lemma below.

Lemma 13. *Let $C_1(\sigma, \kappa)$ be given by (51). Then, for every $\kappa \geq 2$ and all $\sigma \geq 0$, $C_1(\kappa, \sigma) \leq 0$.*

Proof. Let $s(\sigma) = 1 + \tau_0$, with τ_0 given by (49), and note that $\tau_0^2 / (\kappa s(\sigma)^6) > 0$. Thus, the sign of C_1 is the opposite of the sign of $N_{C_1}(s(\sigma) - 1, \kappa)$, where

$$N_{C_1}(t, \kappa) = 4t^4 + (6 - 3\kappa)t^3 - (6 + 3\kappa)t^2 + (\kappa^2 + 9\kappa - 14)t - 3\kappa^2 + 9\kappa - 6.$$

At $\sigma = 0$, one has $s(0) - 1 = \kappa - 1$, and a direct substitution yields $N_{C_1}(\kappa - 1, \kappa) := \kappa^4 - 3\kappa^3 + 2\kappa^2 = \kappa^2(\kappa - 1)(\kappa - 2)$. Moreover, differentiating in t gives $N''_{C_1}(t, \kappa) = 6(-3\kappa t - \kappa + 8t^2 + 6t - 2) > 0$, for all $t \geq \kappa - 1$ and $\kappa \geq 2$, so $N'_{C_1}(\cdot, \kappa)$ is increasing on $[\kappa - 1, \infty)$. As $N'_{C_1}(\kappa - 1, \kappa) = \kappa(\kappa - 2)(7\kappa - 3) \geq 0$, for $\kappa \geq 2$, it follows that $N_{C_1}(\cdot, \kappa)$ is increasing on $[\kappa - 1, \infty)$. Therefore, for every $\sigma \geq 0$,

$$N_{C_1}(s(\sigma) - 1, \kappa) \geq N_{C_1}(\kappa - 1, \kappa) = \kappa^2(\kappa - 1)(\kappa - 2) \geq 0 \quad \text{for } \kappa \geq 2.$$

Since the prefactor is positive, $C_1(\kappa, \sigma) \leq 0$ for all σ as soon as $\kappa \geq 2$. \square

Lemma 14. Let $B_2(\sigma, \kappa)$ be given by (53). Then, for every $\kappa > 1$ and all $\sigma \geq 0$, $B_2(\kappa, \sigma) \leq 0$.

Proof. Recall that

$$B_2(\sigma, \kappa) = -\frac{2\tau_0}{(1+\tau_0)^3} + \frac{2\kappa\tau_0^2}{(1+\tau_0)^3((1+\tau_0)^2 - \kappa)} = \frac{2\tau_0(\kappa - (1+\tau_0))}{(1+\tau_0)^2((1+\tau_0)^2 - \kappa)}.$$

Since $(1+\tau_0)^2 > (1+\tau_0) \geq \kappa$, we have $B_2(\sigma, \kappa) \leq 0$. \square

Lemma 15. Let $C_2(\sigma, \kappa)$ be given by (53). Then, for every $\kappa > 1$ and all $\sigma \geq 0$, $C_2(\kappa, \sigma) \leq 0$.

Proof. Let us again write $s(\sigma) = 1 + \tau_0 > 0$ and note $\tau_0^2 - 1 = (s(\sigma) - 1)^2 - 1 = s(\sigma)^2 - 2s(\sigma)$. Then, substituting and simplifying, we have

$$C_2(\kappa, \sigma) = -\frac{4\tau_0^3}{s(\sigma)^5} + \frac{2\tau_0^3}{s(\sigma)^6} \frac{\kappa(s(\sigma)^2 - 2s(\sigma))}{s(\sigma)^2 - \kappa} = \frac{2\tau_0^3}{s(\sigma)^6} \left(\frac{\kappa s(\sigma)^2 - 2s(\sigma)^3}{s(\sigma)^2 - \kappa} \right) = \frac{2\tau_0^3}{s(\sigma)^4} \frac{\kappa - 2s(\sigma)}{s(\sigma)^2 - \kappa}.$$

Note that $s(\sigma) > \kappa$, and therefore $s(\sigma)^2 - \kappa > 0$ and $\kappa - 2s(\sigma) \leq \kappa - 2\kappa = -\kappa < 0$. Because $\tau_0 > 0$ for $\kappa > 1$, the prefactor $2\tau_0^3/s(\sigma)^4 > 0$. Therefore $C_2(\kappa, \sigma) \leq 0$. \square

Combining the results from Lemmas 12, 13, 14 and 15 concludes the proof of Theorem 4.

D DETAILS FOR THE EXPERIMENTAL SETUP

For both datasets, the curves are obtained by running 100 equally spaced values of λ with the same splits, so that the observations focus on the performativity effect. Data is split uniformly at random across the different steps.

Housing. We keep all features of the dataset and normalize them. We center the target feature since we use a linear regression without intercept. Following Cyffers et al. (2024), we fix the features affected by the performativity effect to be `MedInc`, `AveBedrms`, and `AveOccup`, with all values of b set equal.

LSAC. We keep only one feature in cases of redundant encoding, drop features that are too strongly correlated with the target `GPA` ($\rho > 0.6$), and randomly select roughly half of the features to be affected by the performativity effect. The names of these features are reported in Table 1. We normalize all features and center the target. All coefficients of b are equal.

Table 1: Features of the LSAC dataset

Category	Feature name
Redundant	<code>male</code> (same as <code>sex</code>), <code>parttime</code> (same as <code>fulltime</code>), <code>decile1</code> (same as <code>decile1b</code>)
With $\rho > 0.6$	<code>ugpa</code> , <code>index6040</code> , <code>dnn</code> bar pass prediction
With $b_{\text{feat}} = \bar{b}$	<code>Unnamed0</code> , <code>decile1b</code> , <code>decile3</code> , <code>other</code> , <code>asian</code> , <code>black</code> , <code>hispanic</code> , <code>pass_bar</code> , <code>tier</code>

Reproducibility and LLM Usage We plan to publicly release the code upon acceptance. All experiments were run on a single laptop. Large Language Models were used only for rewording, formatting, basic scripting and documentation.